An Overview of MIMO Communications - A Key to Gigabit Wireless

A. J. Paulraj, D. Gore, R. U. Nabar, and H. Bölcskei

Abstract

High data rate wireless communications, nearing 1 Gigabit/second (Gbps) transmission rates, is of interest in emerging Wireless Local Area Networks (WLANs) and home Audio/Visual (A/V) networks. Designing very high speed wireless links that offer good Quality-of-Service (QoS) and range capability in Non-Line-of-Sight (NLOS) environments constitutes a significant research and engineering challenge. Ignoring fading in NLOS environments, we can, in principle, meet the 1Gbps data rate requirement with a single-transmit single-receive antenna wireless system if the product of bandwidth (measured in Hz) and spectral efficiency (measured in bps/Hz) is equal to 10^9. As we shall outline in this paper, a variety of cost, technology and regulatory constraints make such a brute force solution unattractive if not impossible. The use of multiple antennas at transmitter and receiver, popularly known as multiple-input multiple-output (MIMO) wireless is an emerging cost-effective technology that offers substantial leverages in making 1Gbps wireless links a reality. This paper provides an overview of MIMO wireless technology covering channel models, performance limits, coding, and transceiver design.

Keywords: MIMO, channel models, capacity, space-time coding, spatial multiplexing, receiver design, performance limits, MIMO-OFDM

A. J. Paulraj is with the Information Systems Laboratory, Stanford University, Stanford, CA. E-mail: apaulraj@stanford.edu

D. Gore is with Qualcomm Inc., San Diego, CA. Email: dgore@qualcomm.com

R. U. Nabar and H. Bölcskei are with the Communication Technology Laboratory, Swiss Federal Institute of Technology (ETH) Zurich, Zurich, Switzerland. E-mail: {nabar, boelcskei}@nari.ee.ethz.ch

I. INTRODUCTION

High data rate wireless communications, nearing 1 Gigabit/second (Gbps) transmission rates, is of interest in emerging Wireless Local Area Networks (WLANs) and home Audio/Visual (A/V) networks. Currently, WLANs offer peak rates of 10 Megabits/s (Mbps), with 50Mbps to 100Mbps becoming available soon. However, even 50Mbps is inadequate when faced with the demand for higher access speeds due to the increase in rich media content and competition from 10Gbps wired LANs. Additionally, future home A/V networks will be required to support multiple high speed High Definition Television (HDTV) A/V streams, which again demand near 1Gbps data rates. Another challenge faced by WLANs and home A/V environments as well as outdoor Wireless Wide Area Network (WWAN) systems for fixed/nomadic access is Non-Line-of-Sight (NLOS) propagation, which induces random fluctuations in signal level, known as fading.

Designing very high speed wireless links that offer good Quality-of-Service (QoS) and range capability in NLOS environments constitutes a significant research and engineering challenge. Ignoring fading for the moment, we can, in principle, meet the 1Gbps data rate requirement if the product of bandwidth (measured in Hz) and spectral efficiency (measured in bps/Hz) equals 10^9. As we shall describe in the following, a variety of cost, technology and regulatory constraints make such a brute force solution unattractive, if not impossible. In this paper, we provide an overview of an emerging technology, known as multiple-input multiple-output (MIMO) wireless that offers significant promise in making 1Gbps wireless links in NLOS environments a reality.

Several efforts are currently underway to build sub-Gbps NLOS broadband wireless systems. In WWANs (corresponding standards are currently under development by IEEE 802.16), Iospan Wireless (founded by the first author of this paper and acquired by Intel Corp.) successfully developed a MIMO wireless system (physical layer and medium access control layer technology) using Orthogonal Frequency Division Multiplexing (OFDM) modulation for NLOS environments. The system is designed for a cellular plan with a reuse factor of two and delivers a peak spectral efficiency of 12bps/Hz. Current chipsets offer 13Mbps goodput in a 2MHz channel. Future releases will support a goodput of 45Mbps in a 7MHz channel. The system is aimed at fixed and nomadic/low mobility applications with cell sizes up to 4 miles. In mobile access, there is an effort under the International Telecommunications Union (ITU) working group to

integrate MIMO techniques into the High Speed Downlink Packet Access (HSDPA) channel, which is a part of the Universal Mobile Telecommunications System (UMTS) standard. Lucent Technologies recently announced a chip for MIMO enhancement of UMTS/HSDPA, but has released no further details. Preliminary efforts are also underway to define a MIMO overlay for the IEEE 802.11 standard for WLANs under the newly formed Wireless Next Generation (WNG) group. With the exception of Iospan's product, the other efforts in MIMO technology are expected to take 3-4 years to reach deployment status. These efforts can serve as a good learning base for next generation Gigabit wireless systems. In this paper, we outline the value of MIMO technology in the development of viable Gigabit wireless systems and provide an overview of this technology.

Organization of the paper. The remainder of this paper is organized as follows. Section II discusses the design tradeoffs in building Gigabit wireless systems and highlights the leverages of MIMO technology. Section III introduces a MIMO channel model for NLOS environments. In Section IV, we study the capacity gains resulting from the use of MIMO technology, while Sections V and VI review signaling and receiver design for MIMO systems, respectively. Section VII explores fundamental performance limits in communicating over MIMO channels. In Section VIII, we briefly review MIMO-OFDM, an increasingly popular modulation technique in broadband MIMO wireless channels. We present our conclusions in Section IX.

Notation. The superscripts ^{T}, ^{H} and * stand for transposition, conjugate transposition and elementwise conjugation, respectively. $\mathcal{E}$ denotes the expectation operator while $\star$ is the convolution operator with $h(\tau, t) \star s(t) = \int h(\tau, t)s(t - \tau)d\tau$. $\mathbf{I}_m$ stands for the $m \times m$ identity matrix, $\mathbf{0}$ denotes the all zeros matrix of appropriate dimensions. $\|\mathbf{A}\|_F$, $\det(\mathbf{A})$, and $\mathrm{Tr}(\mathbf{A})$ stand for the Frobenius norm, determinant, and trace respectively, of the matrix $\mathbf{A}$. $\|\mathbf{a}\|$ denotes the Euclidean norm of the vector $\mathbf{a}$. $[\mathbf{A}]_{i,j}$ stands for the element in the i-th row and j-th column of $\mathbf{A}$. For an $m \times n$ matrix $\mathbf{A} = [\mathbf{a}_1\ \mathbf{a}_2\ ...\ \mathbf{a}_n]$, we define the $mn \times 1$ vector $\mathrm{vec}(\mathbf{A}) = [\mathbf{a}_1^T\ \mathbf{a}_2^T\ ...\ \mathbf{a}_n^T]^T$. A complex random variable $Z = X + jY$ is $\mathcal{CN}(0, \sigma^2)$ if X and Y are i.i.d. $\mathcal{N}(0, \sigma^2/2)$.

II. BUILDING GIGABIT WIRELESS LINKS

As noted in the preceding section, we can, in principle, reach 1Gbps link speed in a standard single-input single-output (SISO) wireless link by employing sufficiently high bandwidth along with coding and modulation that achieves the required spectral efficiency. However, there are

several problems with such a simplistic approach.

Let us start by discussing how transmit power and receive signal-to-noise ratio (SNR) constraints limit the maximum achievable spectral efficiency in SISO links. Firstly, the transmit power in a terminal used by or located near human beings is limited to less than 1Watt in indoor environments due to bio-hazard considerations. These limits are about a factor of ten higher in outdoor tower-based base-stations. Secondly, the peak SNR limit in a wireless receiver rarely exceeds 30-35dB because of the difficulty in building (at reasonable cost) highly linear receivers with low phase noise. More generally, the signal-to-noise-and-interference-ratio (SINR) in cellular systems is capped due to the presence of co-channel interference. It is well known that aggressive cellular reuse with a low target SINR is advantageous for achieving high multi-cell spectral efficiency. Also, channel fading in the presence of imperfect power control and peak power limitations at the transmitter results in the peak achievable SINR being lower than the received SNR limit of 30-35dB. The average SINR in a cellular reuse scheme lies in the range of 10-20dB at best. This implies that increasing the spectral efficiency in a SISO NLOS cellular network beyond a peak value of 4-6bps/Hz (average value of 2-4bps/Hz) is not possible. In pure Line-of-Sight (LOS) links, practical SISO systems have reached spectral efficiencies of up to 9bps/Hz. However, such systems rely on fixed point-to-point links with very high gain directional antennas and Fresnel clearance to almost completely eliminate fading. The advantage of high gain antennas in reducing the transmit power constraint is not available in NLOS environments, where large angle spread due to scattering can make such antennas highly inefficient.

Let us next consider the implications of simply using the appropriate bandwidth and spectral efficiency product to achieve 1Gbps date rate. Consider a system that realizes a nominal spectral efficiency of 4bps/Hz over 250MHz bandwidth, so that the data rate is 1Gbps. 250MHz of bandwidth is scarce, if not impossible to obtain, particularly in frequency bands below 6GHz, where NLOS networks are feasible. 250MHz of bandwidth is easier to obtain in the 40GHz frequency range. However, at frequencies higher than 6GHz, the increased shadowing by obstructions in the propagation path render NLOS links unusable. Since transmit power and receive SNR are capped as pointed out above, a 250MHz bandwidth will mean a reduction in range. Assuming a path (propagation) loss exponent of 3.0, the range reduces by a factor of 2 (or cell area by a factor of 4) for every factor of eight increase in bandwidth. Therefore, compared to a 10MHz bandwidth system used today, the range of a 250MHz system will drop by a factor of 3 and the

cell area by a factor of 9. On the positive side, a high bandwidth results in frequency diversity which reduces the fade margin (excess transmit power required) in fading NLOS links. We should finally note that in a cellularized system, a total bandwidth of six to nine times the link bandwidth is needed in order to support a cellular reuse plan. This clearly places impossible bandwidth demands on SISO Gigabit wireless systems.

We summarize our discussion by noting that Gbps wireless links in NLOS (and perhaps cellularized) networks using conventional approaches are in general not feasible due to peak and average SNR limits in practical receivers. Additionally, there is a serious range penalty to be paid for high bandwidth systems. MIMO wireless constitutes a technological breakthrough that will allow Gbps speeds in NLOS wireless networks. The following example is designed to illustrate the performance gains delivered by MIMO. Consider a Rayleigh fading NLOS link with an average receive SNR of 20dB and a constant total transmit power (independent of the number of transmit antennas). Let the coherence bandwidth be 20MHz (typical value for indoor scenarios). The bandwidth needed to ensure 99% link reliability is obtained by computing the 1% outage capacity (see Section IV for details). Fig. 1 plots the bandwidth and range of symmetrical MIMO links (i.e., links with an equal number of transmit and receive antennas, M) needed to support 1Gbps link speed. The range is normalized to unity with reference to a SISO system with 10MHz bandwidth. For $M = 1$, we have a standard SISO link with a required bandwidth of 220MHz, and a reduction in range to 35% of the reference system. On the other hand a 10×10 MIMO system can deliver 1Gbps performance with only 20MHz bandwidth and still support 80% of the reference range. Clearly, MIMO technology offers a substantial performance improvement. Note that a MIMO system does not require additional transmit power or receive SNR to deliver such performance gains. Furthermore, the spectral efficiency achieved over a 20MHz bandwidth by the 10×10 MIMO channel is 50bps/Hz which shows that high transmit power is not necessarily required to reach spectral efficiencies in excess of 10bps/Hz. We note that the downside of using a MIMO system is the increased transceiver complexity.

The performance improvements resulting from the use of MIMO systems are due to *array gain, diversity gain, spatial multiplexing gain*, and *interference reduction*. We briefly review each of these leverages in the following considering a system with M_T transmit and M_R receive antennas.

Array gain. Array gain can be made available through processing at the transmitter and

the receiver and results in an increase in average receive SNR due to a coherent combining effect. Transmit/receive array gain requires channel knowledge in the transmitter and receiver, respectively, and depends on the number of transmit and receive antennas. Channel knowledge in the receiver is typically available whereas channel state information in the transmitter is in general more difficult to maintain.

Diversity gain. Signal power in a wireless channel fluctuates randomly (or fades). Diversity is a powerful technique to mitigate fading in wireless links. Diversity techniques rely on transmitting the signal over multiple (ideally) independently fading paths (in time/frequency/space). Spatial (or antenna) diversity is preferred over time/frequency diversity as it does not incur an expenditure in transmission time or bandwidth. If the $M_T M_R$ links comprising the MIMO channel fade independently and the transmitted signal is suitably constructed, the receiver can combine the arriving signals such that the resultant signal exhibits considerably reduced amplitude variability in comparison to a SISO link and we get $M_T M_R$-th order diversity. Extracting spatial diversity gain in the absence of channel knowledge at the transmitter is possible using suitably designed transmit signals. The corresponding technique is known as space-time coding [1], [2], [3], [4].

Spatial multiplexing gain. MIMO channels offer a linear (in $\min(M_T, M_R)$) increase in capacity for no additional power or bandwidth expenditure [5], [6], [7], [8]. This gain, referred to as spatial multiplexing gain, is realized by transmitting independent data signals from the individual antennas. Under conducive channel conditions, such as rich scattering the receiver can separate the different streams, yielding a linear increase in capacity.

Interference reduction. Co-channel interference arises due to frequency reuse in wireless channels. When multiple antennas are used, the differentiation between the spatial signatures of the desired signal and co-channel signals can be exploited to reduce interference. Interference reduction requires knowledge of the desired signal's channel. Exact knowledge of the interferer's channel may not be necessary. Interference reduction (or avoidance) can also be implemented at the transmitter, where the goal is to minimize the interference energy sent towards the co-channel users while delivering the signal to the desired user. Interference reduction allows aggressive frequency reuse and thereby increases multi-cell capacity.

We note that in general it is not possible to exploit all the leverages of MIMO technology simultaneously due to conflicting demands on the spatial degrees of freedom (or number of antennas). The degree to which these conflicts are resolved depends upon the signaling scheme

and transceiver design.

III. MIMO CHANNEL MODEL

We consider a MIMO channel with M_T transmit and M_R receive antennas. The time-varying channel impulse response between the j-th ($j = 1, 2, \cdots, M_T$) transmit antenna and the i-th ($i = 1, 2, \cdots, M_R$) receive antenna is denoted as $h_{i,j}(\tau, t)$. This is the response at time t to an impulse applied at time $t - \tau$. The composite MIMO channel response is given by the $M_R \times M_T$ matrix $\mathbf{H}(\tau, t)$ with

$$\mathbf{H}(\tau, t) = \begin{bmatrix} h_{1,1}(\tau, t) & h_{1,2}(\tau, t) & \cdots & h_{1,M_T}(\tau, t) \\ h_{2,1}(\tau, t) & h_{2,2}(\tau, t) & \cdots & h_{2,M_T}(\tau, t) \\ \vdots & \vdots & \ddots & \vdots \\ h_{M_R,1}(\tau, t) & h_{M_R,2}(\tau, t) & \cdots & h_{M_R,M_T}(\tau, t) \end{bmatrix}. \tag{1}$$

The vector $[h_{1,j}(\tau, t) \ h_{2,j}(\tau, t) \ \cdots \ h_{M_R,j}(\tau, t)]^T$ is referred to as the spatio-temporal signature induced by the j-th transmit antenna across the receive antenna array. Furthermore, given that the signal $s_j(t)$ is launched from the j-th transmit antenna, the signal received at the i-th receive antenna is given by

$$y_i(t) = \sum_{j=1}^{M_T} h_{i,j}(\tau, t) \star s_j(t) + n_i(t), \ \ i = 1, 2, \cdots, M_R, \tag{2}$$

where $n_i(t)$ is additive noise in the receiver.

Construction of the MIMO channel through a physical scattering model. In the following, we derive a MIMO wireless channel model from a simplistic physical scattering description. For convenience, we suppress the time-varying nature of the channel and use the *narrowband array* assumption described in brief below.

Consider a signal wavefront $\omega(t)$ impinging at angle θ on an antenna array comprising two antennas spaced d apart (see Fig. 2). We assume that the impinging wavefront has a bandwidth of B and is represented as

$$\omega(t) = \beta(t)e^{j\nu_c t}, \tag{3}$$

where $\beta(t)$ is the complex envelope of the signal (with bandwidth B) and ν_c is the carrier frequency in radians.

Under the narrowband assumption, we take the bandwidth B to be much smaller than the reciprocal of the transit time T_ω of the wavefront across the antenna array, i.e., $B \ll \frac{1}{T_\omega}$. Denoting the signal received at the first antenna by $y_1(t)$, the signal received at the second antenna is then given by

$$y_2(t) = y_1(t)e^{-j2\pi \sin(\theta)\frac{d}{\lambda_w}}, \tag{4}$$

where λ_w is the wavelength of the signal wavefront. It is clear from (4) that the signals received at the two antennas are identical, except for a phase shift that depends on the array geometry and the angle of arrival of the wavefront. This result can be extended to arrays with more than two antennas in a straightforward way. We emphasize that the narrowband assumption does not imply that the channel is frequency-flat fading.

We shall next make use of the narrowband assumption in constructing the MIMO channel below. For the sake of simplicity we assume a single bounce based scattering model and consider a scatterer located at angle θ and delay τ with respect to the receive array and with complex amplitude $S(\theta, \tau)$ (see Fig. 3). The same scatterer appears at angle ϕ with respect to the transmit antenna array. Thus, given the overall geometries of transmit and receive arrays, any two of the variables ϕ, θ and τ define the third one. The $M_R \times M_T$ MIMO channel impulse response can now be constructed as (ϕ is a function of θ and τ)

$$\mathbf{H}(\tau) = \int_{-\pi}^{\pi} \int_0^{\tau_{max}} S(\theta, \tau')\mathbf{a}(\theta)\mathbf{b}^T(\phi)g(\tau - \tau')d\tau' d\theta, \tag{5}$$

where τ_{max} is the maximum delay spread in the channel, $g(\tau)$ is the combined response of pulse-shaping at the transmitter and matched-filtering at the receiver and $\mathbf{a}(\theta)$ and $\mathbf{b}(\phi)$ are the $M_R \times 1$ and $M_T \times 1$ array response vectors at the receiver and transmitter, respectively. The single bounce based scattering model in (5) has a number of limitations and cannot adequately model all observed channel effects. A more general model is to assume multiple bounces, i.e., energy from the transmitter uses more than one scatterer to reach the receiver. If we use a double (or multiple) scattering model, the parameters θ, ϕ and τ in (5) become independent of each other.

Classical frequency-flat Rayleigh fading i.i.d. MIMO channel model. Assuming that the delay spread in the channel is small compared to the reciprocal of the signal bandwidth, i.e.,

$\tau_{max} \ll \frac{1}{B}$, we can write (5) as

$$\mathbf{H}(\tau) = \left(\int_{-\pi}^{\pi} \int_0^{\tau_{max}} S(\theta, \tau') \mathbf{a}(\theta) \mathbf{b}^T(\phi) d\tau' d\theta \right) g(\tau) = \mathbf{H} \, g(\tau). \tag{6}$$

Furthermore, we take the combined response $g(\tau)$ to be ideal, so that $g(\tau) = \delta(\tau)$ and hence-forth focus on $\mathbf{H}$ only. With suitable choices of antenna element patterns and array geometry, using a double scattering model, the elements of $\mathbf{H}$ can be assumed to be independent zero mean unit variance circularly symmetric complex Gaussian random variables, i.e., $[\mathbf{H}]_{i,j} (i = 1, 2, \cdots, M_R, \; j = 1, 2, \cdots, M_T) \sim$ i.i.d. $\mathcal{CN}(0, 1)$. Summarizing, we get $\mathbf{H} = \mathbf{H}_w$, the classical i.i.d. frequency-flat Rayleigh fading MIMO channel, which is known to be accurate in NLOS environments with rich scattering and sufficient antenna spacing at transmitter and receiver with all antenna elements identically polarized.

Real-world MIMO channels. In the real world, the statistics of $\mathbf{H}$ can deviate significantly from $\mathbf{H}_w$ due to a variety of reasons including inadequate antenna spacing and/or inadequate scattering leading to spatial fading correlation, the presence of a fixed (possibly LOS) component in the channel resulting in Ricean fading, and gain imbalances between the channel elements through the use of polarized antennas. These effects have been modeled in [8], [9], [10], [11] and have been shown to have a significant impact on the performance limits of MIMO channels. A number of MIMO channel measurements have been carried out across the globe [12], [13], [14], [15], [16], [17]. Fig. 4 shows a measured time-frequency response of an $M_T = M_R = 2$ MIMO channel for a fixed broadband wireless access system at 2.5GHz. Parameters extracted from such measurements include path loss, Ricean K-factor, fading signal correlation, delay spread and Doppler spread. Clearly there is a tremendous variety in real channels. A set of six channels known as the Stanford University Interim (SUI) models [18], reflective of the three terrains (urban, suburban, and hilly) in the continental USA, have been developed and adopted by the IEEE 802.16 standards committee for fixed broadband wireless applications.

Frequency-flat vs. frequency-selective fading. If the bandwidth-delay spread product of the channel satisfies, $B \times \tau_{max} \geq 0.1$, the channel is generally said to be frequency-selective [19]. Otherwise, the channel is said to be frequency-flat. The variation of the matrix-valued transfer function

$$\widetilde{\mathbf{H}}(f) = \int_0^{\infty} \mathbf{H}(\tau) e^{-j2\pi f \tau} d\tau \tag{7}$$

will depend on the delay spread and hence on the coherence bandwidth B_C (approximated by the reciprocal of the delay spread). For frequencies f_1 and f_2 with $|f_1 - f_2| \gg B_C$, we have under Rayleigh fading conditions $\mathcal{E}\{\text{vec}(\widetilde{\mathbf{H}}(f_1))\text{vec}^H(\widetilde{\mathbf{H}}(f_2))\} = \mathbf{0}$, i.e., the channel responses at two frequencies spaced sufficiently apart are uncorrelated. The spatial statistics of $\widetilde{\mathbf{H}}(f)$ will depend on the scattering environment and the array geometry at both the transmitter and receiver. With rich scattering and sufficient antenna spacing, the channel matrix is i.i.d. for all frequencies, i.e., $\widetilde{\mathbf{H}}(f) = \widetilde{\mathbf{H}}_w(f)$. We note, however, that the correlation between the $\widetilde{\mathbf{H}}(f)$ for different frequencies depends on the power delay profile of the channel and the delay spread.

IV. CAPACITY OF MIMO CHANNELS

The Shannon capacity of a communication channel is the maximum asymptotically (in the block-length) error-free transmission rate supported by the channel. In the following, we will examine the capacity benefits of MIMO channels. We begin by introducing the discrete-time (sampled) MIMO input-output signal model.

Discrete-time input-output relation. For the sake of simplicity we assume that the channel is frequency-flat fading (the capacity of frequency-selective fading MIMO channels will be discussed later in this section). The input-output relation over a symbol period assuming single-carrier (SC) modulation is given by

$$\mathbf{y} = \sqrt{\frac{E_s}{M_T}}\mathbf{H}\mathbf{s} + \mathbf{n}, \tag{8}$$

where $\mathbf{y}$ is the $M_R \times 1$ received signal vector, $\mathbf{s}$ with $\mathcal{E}\{\mathbf{s}\} = \mathbf{0}$ is the $M_T \times 1$ transmitted signal vector, $\mathbf{H}$ is the $M_R \times M_T$ MIMO channel matrix, $\mathbf{n}$ is additive temporally white complex Gaussian noise with $\mathcal{E}\{\mathbf{n}\mathbf{n}^H\} = N_o\mathbf{I}_{M_R}$, and E_s is the total average energy available at the transmitter over a symbol period. We constrain the total average transmitted power over a symbol period by assuming that the covariance matrix of $\mathbf{s}$, $\mathbf{R_{ss}} = \mathcal{E}\{\mathbf{s}\mathbf{s}^H\}$, satisfies $\text{Tr}(\mathbf{R_{ss}}) = M_T$.

Capacity of a deterministic MIMO channel. In the following, we assume that the channel $\mathbf{H}$ is perfectly known to the receiver (channel knowledge at the receiver can be maintained via training and tracking). Although $\mathbf{H}$ is random, we shall first study the capacity of a sample realization of the channel, i.e., we consider $\mathbf{H}$ to be deterministic. It is well known that capacity is achieved with Gaussian code books, i.e., $\mathbf{s}$ is a circularly symmetric complex Gaussian vector [7]. For $\mathbf{s}$ Gaussian, the mutual information associated with the channel for a given input covariance

matrix $\mathbf{R_{ss}}$ is given by

$$I = \log_2 \det \left(\mathbf{I}_{M_R} + \frac{E_s}{M_T N_o} \mathbf{H} \mathbf{R_{ss}} \mathbf{H}^H \right) \text{ bps/Hz,}$$

and the capacity of the MIMO channel follows as [7]

$$C = \max_{\mathbf{R_{ss}}} \log_2 \det \left(\mathbf{I}_{M_R} + \frac{E_s}{M_T N_o} \mathbf{H} \mathbf{R_{ss}} \mathbf{H}^H \right) \text{ bps/Hz,} \tag{9}$$

where the maximization is performed over all possible input covariance matrices satisfying $\text{Tr}(\mathbf{R_{ss}}) = M_T$. Furthermore, given a bandwidth of B Hz, the maximum asymptotically (in the block-length) error-free data rate supported by the MIMO channel is simply WC bps.

Acquiring channel knowledge at the transmitter is in general very difficult in practical systems. In the absence of channel state information at the transmitter, it is reasonable to choose s to be spatially white, i.e., $\mathbf{R_{ss}} = \mathbf{I}_{M_T}$. This implies that the signals transmitted from the individual antennas are independent and equi-powered. The mutual information achieved with this covariance matrix is given by [20], [7]

$$I_{CU} = \log_2 \det \left(\mathbf{I}_{M_R} + \frac{E_s}{M_T N_o} \mathbf{H} \mathbf{H}^H \right), \tag{10}$$

which may be decomposed as

$$I_{CU} = \sum_{i=1}^{r} \log_2 \left(1 + \frac{E_s}{M_T N_o} \lambda_i \right), \tag{11}$$

where r is the rank of $\mathbf{H}$ and λ_i $(i = 1, 2, ..., r)$ denote the positive eigenvalues of $\mathbf{H} \mathbf{H}^H$. Clearly, we have $I_{CU} \leq C$. Eq. (11) expresses the spectral efficiency of the MIMO channel as the sum of the capacities of r SISO channels with corresponding channel gains $\sqrt{\lambda_i}$ $(i = 1, 2, ..., r)$ and transmit energy E_s/M_T. It follows that multiple scalar spatial data pipes (also known as spatial modes) open up between transmitter and receiver resulting in significant performance gains over the SISO case. For example, I_{CU} increases by r bps/Hz for every 3dB increase in transmit power (for high transmit power), as opposed to 1bps/Hz in conventional SISO channels. If the channel were known to the transmitter, the individual spatial channel modes can be accessed through linear processing at transmitter and receiver (modal decomposition) following which transmit energy can be allocated optimally across the different modes via the "waterfilling algorithm" [21], [7] so as to maximize the mutual information and achieve the capacity C.

Capacity of fading MIMO channels. We now consider the capacity of fading MIMO channels. In particular, we shall assume $\mathbf{H} = \mathbf{H}_w$ with perfect channel knowledge at the receiver and no channel state information at the transmitter. Furthermore, we assume an ergodic block fading channel model where the channel remains constant over a block of consecutive symbols, and changes in an independent fashion across blocks. The average SNR at each of the receive antennas is given by E_s/N_o, which can be demonstrated as follows. The signal received at the i-th receive antenna is obtained as

$$y_i = \mathbf{h}_i \mathbf{s} + n_i, \tag{12}$$

where the $1 \times M_T$ vector $\mathbf{h}_i$ represents the i-th row of $\mathbf{H}$ and n_i is the i-th element of $\mathbf{n}$. Since $\mathcal{E}\{|h_{i,j}|^2\} = 1$ and $\text{Tr}(\mathbf{R_{ss}}) = E_s$, it follows that $\mathcal{E}\{|y_i|^2\} = E_s + N_o$ and hence the average SNR at the i-th receive antenna is given by $\rho = E_s/N_o$.

We shall see below that in a fading channel there are essentially two notions of capacity – ergodic capacity and outage capacity [22], [23], [7], which relate to the mean and tail behavior of I_{CU}, respectively.

Ergodic capacity: If the transmitted codewords span an infinite number of independently fading blocks, the Shannon capacity also known as ergodic capacity is achieved by choosing $\mathbf{s}$ to be circularly symmetric complex Gaussian with $\mathbf{R_{ss}} = \mathbf{I}_{M_T}$ resulting in [7], [24]

$$C = \mathcal{E}\{I_{CU}\}, \tag{13}$$

where the expectation is with respect to the random channel. It has been established that at high SNR [7], [25]

$$C = \min(M_R, M_T) \log_2 \rho + O(1), \tag{14}$$

which clearly shows the linear increase in capacity in the minimum of the number of transmit and receive antennas. Fig. 5 depicts the ergodic capacity of several MIMO configurations as a function of SNR. As expected, the ergodic capacity increases with increasing ρ and also with M_T and M_R. We note that the ergodic capacity of a SIMO ($M \times 1$) channel is greater than the ergodic capacity of a corresponding MISO ($1 \times M$) channel. This is due to the fact that in the absence of channel knowledge at the transmitter MISO channels do not offer array gain. We refer the interested reader to [24], [26], [27] for analysis of the channel capacity when neither the transmitter nor the receiver knows the channel matrix $\mathbf{H}$.

Outage capacity: In applications where delay is an issue and the transmitted codewords span a single block only, the Shannon capacity is zero. This is due to the fact that no matter how small the rate at which we wish to communicate, there is always a non-zero probability that the given channel realization will not support this rate. We define the $q\%$ outage capacity $C_{out,q}$, as the information rate that is guaranteed for $(100 - q)\%$ of the channel realizations [22], [23], i.e.,

$$P(I_{CU} \leq C_{out,q}) = q\%. \tag{15}$$

Fig. 6 shows the 10% outage capacity for several MIMO configurations as a function of SNR. As in the case of ergodic capacity, we can see that the outage capacity increases with SNR and that MIMO channels yield significant improvements in outage capacity. In fact the behavior of the 10% outage capacity as a function of SNR, M_T and M_R is almost identical to the behavior of ergodic capacity. The outage probability for a given transmission rate R is the probability that the mutual information falls below that rate R, i.e., $P_{out}(R) = P(I_{CU} \leq R)$, and can be interpreted as the packet error rate (PER). This interpretation will lead to an interesting tradeoff between transmission rate and outage probability which we shall explore in greater detail in Section VII.

Capacity of frequency-selective fading MIMO channels. So far, we have restricted our discussion to frequency-flat fading MIMO channels. In the following, we shall briefly discuss frequency-selective fading MIMO channels. The capacity of a frequency-selective fading MIMO channel can be obtained by dividing the frequency band of interest into N sub-channels, each having bandwidth $\frac{B}{N}$ Hz. If N is sufficiently large each sub-channel can be assumed frequency-flat fading (see Fig. 7). Denoting the i-th $M_R \times M_T$ sub-channel as $\mathbf{H}_i$ $(i = 1, 2, \cdots, N)$ and assuming that transmit power is allocated uniformly across space (transmit antennas) and frequency, the mutual information associated with a given realization of the frequency-selective MIMO channel is given by [8]

$$I_{FS} = \frac{1}{N} \sum_{i=1}^{N} \log_2 \det \left(\mathbf{I}_{M_R} + \frac{E_s}{M_T N_o} \mathbf{H}_i \mathbf{H}_i^H \right) \text{ bps/Hz}, \tag{16}$$

where E_s is the energy allocated to the i-th sub-channel.

The ergodic capacity of the frequency-selective fading MIMO channel is given by

$$C_{FS} = \mathcal{E}\{I_{FS}\}. \tag{17}$$

The outage capacity follows from the corresponding definition for the frequency-flat case. Note that the outage capacity (at low outage rates) of the frequency-selective fading channel will in general be higher than the outage capacity of a frequency-flat fading channel. This is due to frequency diversity which leads to increased tightening (the cumulative distribution function (CDF) becomes increasingly step-like) of the probability density function (PDF) of mutual information. Fig. 8 illustrates this effect by showing the CDF of the mutual information of a frequency-selective fading MIMO channel with $M_T = M_R = 2$, for increasing number of degrees of freedom[1] $L = B/B_C$ (and hence increasing frequency diversity). The CDF of mutual information approaches a step function improving outage capacity at low outage rates. The influence of physical parameters such as delay spread, cluster angle spread and total angle spread on ergodic and outage capacity of frequency-selective fading MIMO channels has been studied in detail in [8].

V. MIMO SIGNALING

In this section, we review some basic MIMO signaling techniques We start by describing the framework employed in the remainder of this section. Consider the schematic in Fig. 9 where qK information bits are input to a block that performs the functions of forward-error-correction (temporal) encoding, symbol mapping and interleaving. In the process $q(N - K)$ parity bits are added resulting in N data symbols at the output with constellation size 2^q (for example, $2^q = 4$ if 4-QAM modulation is employed). The resulting block of N data symbols is then input to a space-time encoder that adds an additional $M_T T - N$ parity data symbols and packs the resulting $M_T T$ symbols into an $M_T \times T$ matrix (or frame) of length T. This frame is then transmitted over T symbol periods and is referred to as the space-time codeword. The signaling (data) rate on the channel is qK/T bps/Hz, which should not exceed the channel capacity if we wish to signal asymptotically error-free. Note that we can rewrite the signaling rate as

$$\frac{qK}{T} = q \left(\frac{qK}{qN} \right) \left(\frac{N}{T} \right)$$

$$= q \, r_t \, r_s,$$

(18)

where $r_t = qK/qN$ is the (temporal) code rate of the outer encoder, while $r_s = N/T$ is the spatial code rate [3], defined as the number of independent data symbols in a space-time

---

[1]A uniform power delay profile was assumed in this example.

codeword divided by the frame length. Depending on the choice of the spatial signaling mode, the spatial rate varies between 0 and M_T. For certain classes of space-time codes, discussed below, such as space-time trellis codes, the functions of the symbol mapper and space-time encoder are combined into a single block. In the following, we briefly discuss two space-time coding techniques – space-time diversity coding ($r_s \leq 1$) and spatial multiplexing ($r_s = M_T$). Throughout this section we focus on the case where the transmitter does not have channel state information and the receiver knows the channel perfectly. For a discussion of the non-coherent case where neither the transmitter nor the receiver know the channel, the interested reader is referred to [24], [26], [28].

A. Space-Time Diversity Coding

The objective of space-time diversity coding is to extract the total available spatial diversity in the MIMO channel through appropriate construction of the transmitted space-time codewords. As examples we consider two specific diversity coding techniques, the Alamouti scheme [2] and delay diversity [29], both of which realize full spatial diversity (without requiring channel knowledge at the transmitter).

Alamouti scheme. Consider a MIMO channel with two transmit antennas and any number of receive antennas. The Alamouti transmission technique is as follows: two different data symbols s_1 and s_2 are transmitted simultaneously from antennas 1 and 2, respectively, during the first symbol period, following which symbols $-s_2^*$ and s_1^* are launched from antennas 1 and 2, respectively (see Fig. 10). Note that $r_s = 1$ (two independent data symbols are transmitted over two symbol periods) for the Alamouti scheme.

We assume that the channel is i.i.d. frequency-flat fading with $h_1, h_2 \sim \mathcal{CN}(0,1)$ and remains constant over (at least) two consecutive symbol periods. Appropriate processing (details can be found in [2]) at the receiver collapses the vector channel into a scalar channel for either of the transmitted data symbols such that

$$z_i = \sqrt{\frac{E_s}{2}} \|\mathbf{H}\|_F^2 s_i + \tilde{n}_i, \ \ i = 1, 2, \tag{19}$$

where z_i is the processed received signal corresponding to transmitted symbol s_i and $\tilde{n}_i \sim \mathcal{CN}(0, \|\mathbf{H}\|_F^2 N_o)$ is scalar processed noise. Even though channel knowledge is not available to the transmitter, the Alamouti scheme extracts $2M_R$-th order diversity. We note, however, that (as

shown in Fig. 11) array gain is realized only at the receiver (recall that the transmitter does not have channel state information). The Alamouti scheme may be extended to channels with more than two transmit antennas through orthogonal space-time block coding (OSTBC) [4] albeit at a loss in spatial rate (i.e., $r_s < 1$). However, the low decoding complexity of OSTBC renders this technique highly attractive for practical applications.

Delay diversity. The second simple scheme for space-time diversity coding we want to discuss is delay diversity [29] which converts spatial diversity into frequency diversity by transmitting the data signal from the first antenna and a delayed replica thereof from the second antenna (see Fig. 12). Retaining the assumption that $M_T = 2$ and $M_R = 1$ and assuming that the delay induced by the second antenna equals one symbol period, the effective channel seen by the data signal is a frequency-selective fading SISO channel with impulse response

$$h[k] = h_1\delta[k] + h_2\delta[k-1], \tag{20}$$

where h_1 and h_2 are as defined above. We note that the effective channel in (20) looks exactly like a two-path (symbol spaced) SISO channel with independently fading paths and equal average path energy. A maximum-likelihood (ML) detector will therefore realize full second-order diversity at the receiver.

General space-time diversity coding techniques. The general case of space-time codeword construction for achieving full ($M_R M_T$-th order) diversity gain has been studied in [3] and leads to the well known rank and determinant criteria. Extensions of these design criteria to the frequency-selective fading case can be found in [30], [31].

B. Spatial Multiplexing

The objective of spatial multiplexing as opposed to space-time diversity coding is to maximize transmission rate. Accordingly, M_T independent data symbols are transmitted per symbol period so that $r_s = M_T$. In the following, we describe several encoding options that can be used in conjunction with spatial multiplexing.

Horizontal encoding (HE). The bit stream to be transmitted is first demultiplexed into M_T separate data streams (see Fig. 13). Each stream undergoes independent temporal encoding, symbol mapping and interleaving and is then transmitted from the corresponding antennas. The antenna-stream association remains fixed over time. The spatial rate is clearly $r_s = M_T$ and the

overall signaling rate is therefore given by qr_tM_T bps/Hz. The HE scheme can at most achieve M_R-th order diversity, since any given symbol is transmitted from only one transmit antenna and received by M_R receive antennas. As we shall see below, this is a source of sub-optimality of the HE architecture but it does simplify receiver design. The coding gain achieved by HE depends on the coding gain of the temporal code. Finally, we note that a maximum array gain of M_R can be realized.

Vertical encoding (VE). In this architecture the bit stream undergoes temporal encoding symbol mapping and interleaving after which it is demultiplexed into M_T streams transmitted from the individual antennas (see Fig. 14). This form of encoding can achieve full (M_TM_R-th order) diversity gain (provided the temporal code is designed properly) since each information bit can be spread across all the transmit antennas. However, VE requires joint decoding of the sub-streams which increases receiver complexity compared to HE where the individual data streams can be decoded separately. The spatial rate of VE is $r_s = M_T$ and the overall signaling rate is given by qr_tM_T bps/Hz. The coding gain achieved by VE will depend on the temporal code and a maximum array gain of M_R can be achieved.

Combinations of HE and VE. Various combinations/variations of the above two encoding strategies are possible. One such transmission technique is Diagonal Encoding (DE) where the incoming data stream first undergoes HE after which the antenna-stream association is rotated in a round-robin fashion. Making the codewords long enough ensures that each codeword is transmitted from all M_T antennas so that full (M_TM_R-th order) diversity gain can be achieved. The distinguishing feature of DE is the fact that at full spatial rate of M_T and full diversity gain of order M_TM_R, the system retains the decoding complexity of HE. The Diagonal-Bell Labs Layered Space Time Architecture (D-BLAST) [6] transmission technique follows a diagonal encoding strategy with an initial wasted space-time triangular block, where no transmission takes place. This initial wastage is required to ensure optimality of the (low complexity) stream-by-stream decoding algorithm. Especially for short block lengths the space-time wastage results in a non-negligible rate loss which constitutes a major drawback of DE. Finally, we note that DE can achieve a maximum array gain of M_R.

VI. MIMO RECEIVER ARCHITECTURES

In this section, we shall discuss receiver architectures for space-time diversity coding ($r_s \leq 1$) and spatial multiplexing ($r_s = M_T$).

A. Receivers for Space-Time Diversity Coding

OSTBC decouples the vector detection problem into scalar detection problems [4]. Similar extensions can be made to frequency-selective fading MIMO channels [32]. Hence, receiver techniques (that have been studied in detail) such as zero-forcing (ZF), minimum-mean square error estimation (MMSE) and (optimal) maximum-likelihood sequence estimation (MLSE) can be applied directly. Transmit diversity techniques such as delay diversity [29] and frequency offset diversity [33] collapse the MISO channel into a SISO channel and hence also allow the application of SISO receiver architectures. For a general space-time trellis code [3], a vector Viterbi decoder has to be employed. Space-time trellis coding in general provides improved performance over OSTBC at the expense of receiver complexity.

B. Receivers for Spatial Multiplexing

The remainder of this section focuses on receiver structures for spatial multiplexing and the corresponding performance-complexity tradeoff. The problem faced by a receiver for spatial multiplexing is the presence of multi-stream interference (MSI), since the signals launched from the different transmit antennas interfere with each other (recall that in spatial multiplexing the different data streams are transmitted co-channel and hence occupy the same resources in time and frequency). For the sake of simplicity we restrict our attention to the case $M_R \geq M_T$.

Maximum-likelihood (ML) receiver. The ML receiver performs vector decoding and is optimal in the sense of minimizing the error probability. Assuming equally likely, temporally uncoded vector symbols, the ML receiver forms its estimate of the transmitted signal vector according to

$$\widehat{\mathbf{s}} = \arg\min_{\mathbf{s}} \left\| \mathbf{y} - \sqrt{\frac{E_s}{M_T}} \mathbf{H} \mathbf{s} \right\|^2, \tag{21}$$

where the minimization is performed over all possible transmit vector symbols $\mathbf{s}$. Denoting the alphabet size of the scalar constellation transmitted from each antenna by $\mathcal{A}$, a brute force

implementation requires an exhaustive search over a total of $\mathcal{A}^{M_T}$ vector symbols rendering the decoding complexity of this receiver exponential in the number of transmit antennas. However, the recent development of fast algorithms [34], [35], [36] for sphere decoding techniques [37] offers promise to reduce computational complexity significantly (at least for lattice codes). As already pointed out above, the ML receiver realizes M_R-th order diversity for HE and (full) $M_T M_R$-th order diversity for VE and DE.

Linear receivers. We can reduce the decoding complexity of the ML receiver significantly by employing linear receiver front-ends (see Fig. 15) to separate the transmitted data streams, and then independently decode each of the streams. We discuss the zero-forcing (ZF) and minimum mean squared error (MMSE) linear front-ends below.

ZF receiver: The ZF front-end is given by

$$\mathbf{G}_{ZF} = \sqrt{\frac{M_T}{E_s}}\,\mathbf{H}^\dagger, \tag{22}$$

where $\mathbf{H}^\dagger = (\mathbf{H}^H\mathbf{H})^{-1}\mathbf{H}^H$ denotes the Moore-Penrose inverse of the channel matrix $\mathbf{H}$. The output of the ZF receiver is obtained as

$$\mathbf{z} = \mathbf{s} + \sqrt{\frac{M_T}{E_s}}\mathbf{H}^\dagger\mathbf{n}, \tag{23}$$

which shows that the ZF front-end decouples the matrix channel into M_T parallel scalar channels with additive spatially-colored noise. Each scalar channel is then decoded independently ignoring noise correlation across the processed streams. The ZF receiver converts the joint decoding problem into M_T single stream decoding problems (i.e., it eliminates MSI) thereby significantly reducing receiver complexity. This complexity reduction comes, however, at the expense of noise enhancement which in general results in a significant performance degradation (compared to the ML decoder). The diversity order achieved by each of the individual data streams equals $M_R - M_T + 1$ [38], [39].

MMSE Receiver: The MMSE receiver front-end balances MSI mitigation with noise enhancement and is given by

$$\mathbf{G}_{MMSE} = \sqrt{\frac{M_T}{E_s}}\left(\mathbf{H}^H\mathbf{H} + \frac{M_T N_o}{E_s}\mathbf{I}_{M_T}\right)^{-1}\mathbf{H}^H. \tag{24}$$

In the low-SNR regime ($E_s/N_o \ll 1$), the MMSE receiver approaches the matched-filter receiver given by

$$\mathbf{G}_{MMSE} = N_o^{-1}\sqrt{\frac{E_s}{M_T}}\,\mathbf{H}^H \tag{25}$$

and outperforms the ZF front-end (that continues to enhance noise). At high SNR ($E_s/N_o \gg 1$)

$$\mathbf{G}_{MMSE} = \mathbf{G}_{ZF}, \tag{26}$$

i.e., the MMSE receiver approaches the ZF receiver and therefore realizes $(M_R - M_T + 1)$-th order diversity for each data stream.

Successive cancellation receivers. The key idea in a successive cancellation (SUC) receiver is layer peeling where the individual data streams are successively decoded and stripped away layer-by-layer. The algorithm starts by detecting an arbitrarily chosen data symbol (using ZF or MMSE) assuming that the other symbols are interference. Upon detection of the chosen symbol, its contribution from the received signal vector is subtracted and the procedure is repeated until all symbols are detected. In the absence of error propagation SUC converts the MIMO channel into a set of parallel SISO channels with increasing diversity order at each successive stage [20], [40]. In practice, error propagation will be encountered, especially so if there is inadequate temporal coding for each layer. The error rate performance will therefore be dominated by the first stream decoded by the receiver (which is also the stream experiencing the smallest diversity order).

Ordered successive cancellation receivers. An improved SUC receiver is obtained by selecting the stream with the highest SINR at each decoding stage. Such receivers are known as ordered successive cancellation (OSUC) receivers or in the MIMO literature as V-BLAST [41], [42]. OSUC receivers reduce the probability of error propagation by realizing a selection diversity gain at each decoding step. The OSUC algorithm requires slightly higher complexity than the SUC algorithm resulting from the need to compute and compare the SINRs of the remaining streams at each stage.

Numerical comparison. Fig. 16 compares the performance of various receivers for uncoded spatial multiplexing with 4-QAM modulation, $M_T = M_R = 2$ and $\mathbf{H} = \mathbf{H}_w$. The symbol error rate curve for receive diversity with $M_T = 1$ and $M_R = 2$ is plotted for comparison. OSUC is markedly better than SUC which is slightly better than MMSE, but still shows a significant performance degradation in the high-SNR regime when compared to the ML receiver. More specifically, we can see that the ML receiver achieves a diversity order of M_R (reflected by the slope of the error rate curve), the MMSE receiver realizes a diversity order of $M_R - M_T + 1$ (at high SNR) and the OSUC receiver yields a diversity order that lies between $M_R - M_T + 1$ and

M_R.

Table I summarizes the performance features of various receivers with uncoded SM. The ZF, MMSE and SUC receivers provide only $(M_R - M_T + 1)$-th order diversity but have varying SNR loss. The OSUC receiver may realize more than $(M_R - M_T + 1)$-th order diversity because of the ordering (selection) process. The ML receiver is optimal and realizes diversity order M_R.

VII. FUNDAMENTAL PERFORMANCE LIMITS

In this section, we shall examine the fundamental tradeoffs between transmission rate, error rate, and SNR for the case where the transmitter has no channel knowledge and the receiver has perfect channel state information. We assume that the MIMO channel is block fading and that the length of the transmitted codewords is less than or equal to the channel block length. If the channel $\mathbf{H}$ were perfectly known to the transmitter, we could choose a signaling rate equal to or less than channel capacity and guarantee (asymptotically) error-free transmission. The coding scheme to achieve capacity consists of performing modal decomposition [7] which decouples the MIMO channel into parallel SISO channels and then using ideal SISO channel coding. In practice turbo codes should get us very close to the MIMO channel capacity.

If the channel is unknown to the transmitter, modal decomposition is not possible. Furthermore, since the channel is drawn randomly according to a given fading distribution there will always be a non-zero probability that a given transmission rate (no matter how small) is not supported by the channel. We assume that the transmitted codeword (packet) is decoded successfully if the rate is at or below the mutual information (assuming a spatially white transmit covariance matrix) associated with the given channel realization. A decoding error is declared if the rate exceeds the mutual information. Hence, if the transmitter does not know the channel, the packet error rate (PER) will equal the outage probability (as defined in (15)) associated with the transmission rate. According to [43], we define the diversity order for a given transmission rate R as

$$d(R) = - \lim_{\rho \to \infty} \frac{\log(P_e(R, \rho))}{\log \rho}, \tag{27}$$

where $P_e(R, \rho)$ is the PER corresponding to transmission rate R and SNR ρ. Hence, the diversity order is the magnitude of the slope of the PER plotted as a function of the SNR on a log-log scale.

Rate vs. PER vs. SNR for optimal coding. For the sake of clarity of exposition we consider a simple example with $\mathbf{H} = \mathbf{H}_w$ and $M_T = M_R = 2$. We assume that the transmitter has

no knowledge of the channel other than the SNR ρ. A reasonable strategy for the transmitter is to compute the CDF of mutual information for this SNR, and choose the signaling rate for which the PER (i.e., outage probability) is at the desired level. A discussion of the corresponding relations between signaling rate, PER and SNR follows.

Transmission rate fixed. Fig. 17 plots the PER as a function of SNR for a fixed transmission rate of 6bps/Hz. The magnitude of the slope of the PER curve has been shown to be $M_T M_R$ [43] for a fixed rate and at high enough SNR. This indicates that for fixed rate transmission, optimal coding yields full $M_T M_R$-th order spatial diversity inherent in the channel. In comparison, the PER curve for a SISO AWGN channel with a signaling rate of 6bps/Hz is a vertical line at $\rho = 18$ dB, i.e., an error is always made if we attempt to transmit at 6bps/Hz over the SISO AWGN channel when $\rho < 18$ dB. The result confirms the notion that an AWGN channel has infinite diversity [44] and furthermore shows that for SNR below 18dB, the MIMO fading channel has better performance in terms of PER than the SISO AWGN channel.

PER fixed. Next, keeping the PER fixed at 10%, Fig. 18 plots the outage capacity vs. SNR. We notice that at high SNR the outage capacity increases by $M_T = M_R = 2$ bps/Hz for every 3dB increase in SNR. In general, the magnitude of the slope of the outage capacity vs. SNR curve is $\min(M_T, M_R)$bps/Hz/3db [43]. We can therefore conclude that for fixed PER, using optimal coding, an increase in SNR can be leveraged to increase transmission rate at $\min(M_T, M_R)$bps/Hz/3db.

Achievable rate, PER, and SNR region. Fig. 19 shows the three-dimensional surface of rate vs. PER vs. SNR. The surface represents a fundamental limit for signaling over fading MIMO channels, assuming optimal coding (possibly a D-BLAST like framework) with a large enough block length. The region to the right of this surface is achievable in the sense that it contains triplets of rate, PER and SNR that can be realized. To summarize, with optimal coding for a fixed transmission rate, we can trade an increase in SNR for a reduction in PER (diversity gain equal to $M_T M_R$), and conversely for a fixed PER, we can trade an increase in SNR for a linear increase in rate (at $\min(M_T, M_R)$ bps/Hz/3dB).

Rate vs. PER vs. SNR for sub-optimal coding and receivers. We shall next discuss the Rate vs. PER vs. SNR tradeoff for two sub-optimal coding and associated receiver schemes. In both schemes the MIMO channel is collapsed by the coding scheme into one or more parallel SISO channels through linear pre- and post-processing. The maximum asymptotically (in the block

length) error-free transmission rate supported by this modified MIMO channel is then given by the sum of the capacities of the resulting parallel SISO channels.

(i) OSTBC with ML receiver: As discussed earlier OSTBC guarantees full spatial diversity gain. The effective channel is SISO with post-processing SNR equal to $\frac{\rho}{M_T}\|\mathbf{H}\|_F^2$. The mutual information associated with a given realization of the MIMO channel in conjunction with OSTBC is given by [45]

$$I_{OSTBC} = r_s \log_2 \left(1 + \frac{\rho}{M_T}\|\mathbf{H}\|_F^2 \right) \text{ bps/Hz,} \tag{28}$$

where r_s is the spatial rate of the code. Note that $I_{OSTBC} \leq I_{CU}$, with equality only if every realization of the MIMO channel has rank 1 and $r_s = 1$ [46].

(ii) Spatial multiplexing with HE and MMSE receiver: In spatial multiplexing with HE, the incoming data stream is demultiplexed into M_T equal rate streams, which are subsequently encoded and transmitted from the corresponding antenna (see Fig. 13). At the receiver, the M_T data streams are first separated using an MMSE front-end and then decoded independently. The resulting decoded data streams are then multiplexed into a single stream. The composite stream is guaranteed to be decoded correctly only when the packet corresponding to the stream with the lowest SINR is decoded correctly. Furthermore, since the different streams have equal rate, the total rate is constrained by the weakest stream, i.e., the stream with the lowest SINR. Hence, the mutual information associated with this architecture is given by [45]

$$I_{SM-HE} = M_T \log_2(1 + \min(\eta_1, \eta_2, \cdots, \eta_{M_T})) \text{ bps/Hz,} \tag{29}$$

where η_i is the post-processing SINR for the i-th ($i = 1, 2, \cdots, M_T$) data stream.

Fig. 20 plots the Rate vs. PER vs. SNR tradeoff surface for both schemes described above assuming an i.i.d. MIMO channel with $M_T = M_R = 2$. Comparing with Fig. 19 we can verify that these curves indeed lie in the achievable region. Moreover Fig. 20 shows that the two schemes exhibit significantly different Rate vs. PER vs. SNR tradeoffs. In order to get better insight, Fig. 21 plots a PER vs. SNR slice of Fig. 20 with the signaling rate kept fixed at 6bps/Hz. The same slice for the optimal surface is depicted for comparison. Note that the magnitude of the slope of the SM-HE curve is smaller than that for the curve corresponding to OSTBC, which extracts full diversity gain. Furthermore, at low SNR, SM-HE outperforms the Alamouti scheme. However, due to the higher diversity gain of the Alamouti scheme, at high SNR the situation

reverses. We can see that the question of which scheme to use depends significantly on the target PER and the operational SNR.

VIII. MIMO-OFDM

So far we discussed signaling techniques for frequency-flat fading MIMO channels. Broadband wireless systems, however, encounter large delay spread, and therefore have to cope with frequency-selectivity. In the following, we shall discuss the basic principles of MIMO-OFDM, a particularly attractive modulation scheme in frequency-selective fading channels. We start with the signal model.

Denoting the discrete-time index by k, the input-output relation for the broadband MIMO channel is given by

$$\mathbf{y}[k] = \sum_{l=0}^{L-1} \sqrt{\frac{E_s}{M_T}} \mathbf{H}_l \mathbf{s}[k-l] + \mathbf{n}[k],$$

where $\mathbf{y}[k]$ denotes the $M_R \times 1$ received signal vector, $\mathbf{H}_l$ $(l = 0, 1, ..., L-1)$ is the $M_R \times M_T$ matrix-valued channel impulse response, $\mathbf{s}[k]$ is the $M_T \times 1$ transmit signal vector sequence and $\mathbf{n}[k]$ is the $M_R \times 1$ spatio-temporally white Gaussian noise vector with $\mathcal{E}\{\mathbf{n}[k]\mathbf{n}^H[l]\} = N_o \delta[k-l]$.

The computational complexity of ML detection (or even sub-optimal detection schemes) needed for MIMO-SC modulation is prohibitive since it grows exponentially with the bandwidth-delay spread product. OFDM (Orthogonal Frequency Division Multiplexing) constitutes an attractive alternative modulation scheme which avoids temporal equalization altogether at the cost of a small penalty in channel capacity.

Fig. 22 shows a schematic of OFDM transmission over a SISO channel. An Inverse Fast Fourier Transform (IFFT) operation (on blocks of N data symbols) is performed at the transmitter, following which a cyclic prefix (CP) of length L containing a copy of the first L samples of the parallel-to-serial converted output of the IFFT block is prepended. At the receiver, the CP is removed following which a length N FFT is performed on the received signal sequence. The net result is that the frequency-selective fading channel (of bandwidth B) is decomposed into N parallel frequency-flat fading channels, each having bandwidth B/N.

OFDM extends directly to MIMO channels [47], [48], [8] with the IFFT/FFT and CP operations being performed at each of the transmit and receive antennas. The use of MIMO-OFDM decouples the frequency-selective MIMO channel into a set of N parallel MIMO channels with

the input-output relation for the i-th ($i = 0, 1, ..., N - 1$) tone given by [47], [8]

$$\widetilde{\mathbf{y}}_i = \sqrt{\frac{E_s}{M_T}}\widetilde{\mathbf{H}}_i\widetilde{\mathbf{s}}_i + \widetilde{\mathbf{n}}_i, \tag{30}$$

where $\widetilde{\mathbf{y}}_i$ is the $M_R \times 1$ received signal vector, $\widetilde{\mathbf{H}}_i = \sum_{l=0}^{L-1} \mathbf{H}_l e^{-j\frac{2\pi}{N}li}$ is the $M_R \times M_T$ frequency response, $\widetilde{\mathbf{s}}_i$ is the $M_T \times 1$ transmit signal vector with $\mathcal{E}\{\widetilde{\mathbf{s}}_i\widetilde{\mathbf{s}}_i^H\} = \mathbf{I}_{M_T}$, and $\widetilde{\mathbf{n}}_i$ is $M_R \times 1$ complex Gaussian noise with $\mathcal{E}\{\widetilde{\mathbf{n}}_i\widetilde{\mathbf{n}}_i\}^H = N_o\mathbf{I}_{M_R}$ (and uncorrelated across tones). We note that (30) holds true if the length of the CP satisfies $L_{CP} \geq L$. The loss in spectral efficiency due to the use of a CP is given by $L_{CP}/(N + L_{CP})$ and becomes negligible for $N \gg L_{CP} \geq L$.

Signaling and receivers for MIMO-OFDM. MIMO signaling for SC modulation in frequency-flat fading channels, discussed in Section V, can be overlayed easily on OFDM by simply performing operations on a tone-by-tone basis. In the following, we briefly describe how spatial diversity coding and spatial multiplexing can be extended to MIMO-OFDM and conclude with a short discussion on space-frequency coded MIMO-OFDM where the objective is to realize both spatial and frequency diversity gains.

(i) Spatial diversity coding for MIMO-OFDM: Let us consider, for example, a system with $M_T = 2$ employing the Alamouti scheme ($r_s = 1$), which realizes full spatial diversity gain in the absence of channel knowledge at the transmitter. Recall that implementation of the Alamouti scheme requires that the channel remains constant over at least two consecutive symbol periods. In the OFDM context, assuming that coding is performed over frequency rather than time, this condition translates to the channel remaining constant over at least two consecutive tones. If the delay spread is small, this is a realistic assumption to make. Next, consider two data symbols s_1 and s_2, to be transmitted over two consecutive OFDM tones, i and $i + 1$, using the Alamouti scheme. Symbols s_1 and s_2 are transmitted over antennas 1 and 2, respectively, on tone i, whereas $-s_2^*$ and s_1^* are transmitted over antennas 1 and 2, respectively, on tone $i + 1$ within the same OFDM symbol. The receiver detects the transmitted symbols from the signal received on the two tones using the Alamouti detection technique [2]. As discussed in Section V, the vector detection problem collapses into two scalar detection problems and the Alamouti scheme realizes full spatial diversity gain of order $2M_R$. Note that we do not necessarily have to use consecutive tones, any pair of tones can be used as long as the associated channels are equal. The technique can be generalized to extract spatial diversity in systems with more than 2 transmit antennas by using OSTBC developed for SC modulation in frequency-flat fading channels. We

note, however, that the channel is required to remain constant over at least M_T consecutive OFDM tones (or M_T arbitrarily chosen tones). This assumption will be violated for increasing delay spread. In [30] it was shown that OSTBC achieves full spatial diversity gain even if the delay spread is large. However, the associated ML vector detection problem no longer decouples into scalar detection problems thereby increasing receiver complexity [30]. We finally note that an alternative technique consists of using spatial diversity coding on a per-tone basis across OFDM symbols in time [49]. However, this requires that the channel remains constant over consecutive OFDM symbol periods, which is usually not the case due to the long duration of an OFDM symbol.

(ii) Spatial multiplexing for MIMO-OFDM: Analogous to spatial multiplexing for frequency-flat fading MIMO channels with SC modulation, the objective of spatial multiplexing in conjunction with MIMO-OFDM, is to maximize spatial rate ($r_s = M_T$) by transmitting independent data streams over different antennas [8]. Thus spatial multiplexing in MIMO-OFDM systems reduces to spatial multiplexing over each tone with the choice of receiver architectures being identical to that for frequency-flat fading MIMO channels with SC modulation.

(iii) Space-frequency coded MIMO-OFDM: The spatial diversity coding techniques discussed in (i) realize spatial diversity gain in a MIMO-OFDM system. However OFDM tones with spacing larger than the coherence bandwidth B_C of the channel experience independent fading so that frequency diversity is also available. Denoting the number of coherence bandwidths by $D_{eff} = B/B_C$ it has been shown in [30] that the total diversity gain that can be realized in a MIMO-OFDM systems equals $M_T M_R D_{eff}$. Space-time diversity coding and spatial multiplexing on a tone-by-tone basis with no redundancy introduced across tones will in general not exploit any frequency diversity [30]. In order to extract full spatial as well as frequency diversity, data must be suitably spread across space and frequency [30], [31], [50], [51].

Typically, the bit stream to be transmitted is first encoded, then modulated and interleaved. The resulting data symbols to be transmitted are mapped across space and frequency by a space-frequency encoder such as the one described in [52], [53] for example. The receiver demodulates the received signal and estimates the transmitted space-frequency codeword followed by deinterleaving and decoding. The interested reader is referred to [30], [31], [48], [50], [54], [55] for further details on space-frequency coded MIMO-OFDM.

IX. CONCLUSION

We provided a brief overview of MIMO wireless technology covering channel models, capacity, coding, receiver design, performance limits and MIMO-OFDM. The field is attracting considerable research attention in all of these areas. Significant efforts are underway to develop and standardize channel models for different systems and applications. Understanding the information-theoretic performance limits of MIMO systems, particularly in the multi-user context, is an active area of research. Space-time code and receiver design with particular focus on iterative decoding and sphere decoding allowing low complexity implementation have attracted significant interest recently. Finally, we feel that a better understanding of the system design implications of fundamental performance tradeoffs (such as Rate vs. PER vs. SNR) is required.

From a practical viewpoint, there seems to be enough understanding to build robust MIMO-based wireless solutions that address all layers of a wireless network in an integrated manner (witness Iospan Wireless). The evolution of MIMO from broadband ($\leq$ 10Mbps) to Gbps rates should only be a matter of time as hardware for multi-channel radio-frequency (RF) chains and Digital Signal Processors (DSPs) becomes more affordable.

REFERENCES

[1] J. Guey, M. P. Fitz, M. R. Bell, and W. Kuo, "Signal design for transmitter diversity wireless communication systems over Rayleigh fading channels," in *Proc. IEEE VTC*, vol. 1, Atlanta, GA, Apr./May 1996, pp. 136–140.

[2] S. M. Alamouti, "A simple transmit diversity technique for wireless communications," *IEEE J. Sel. Areas Comm.*, vol. 16, no. 8, pp. 1451–1458, Oct. 1998.

[3] V. Tarokh, N. Seshadri, and A. R. Calderbank, "Space-time codes for high data rate wireless communication: Performance criterion and code construction," *IEEE Trans. Inf. Theory*, vol. 44, no. 2, pp. 744–765, March 1998.

[4] V. Tarokh, H. Jafarkhani, and A. Calderbank, "Space-time block codes from orthogonal designs," *IEEE Trans. Inf. Theory*, vol. 45, no. 5, pp. 1456–1467, July 1999.

[5] A. J. Paulraj and T. Kailath, "Increasing capacity in wireless broadcast systems using distributed transmission/directional reception," *U. S. Patent*, no. 5,345,599, 1994.

[6] G. J. Foschini, "Layered space-time architecture for wireless communication in a fading environment when using multi-element antennas," *Bell Labs Tech. J.*, pp. 41–59, 1996.

[7] I. E. Telatar, "Capacity of multi-antenna Gaussian channels," *European Trans. Tel.*, vol. 10, no. 6, pp. 585–595, Nov./Dec. 1999.

[8] H. Bölcskei, D. Gesbert, and A. J. Paulraj, "On the capacity of OFDM-based spatial multiplexing systems," *IEEE Trans. Comm.*, vol. 50, no. 2, pp. 225–234, Feb. 2002.

[9] D. Gesbert, H. Bölcskei, D. A. Gore, and A. J. Paulraj, "Outdoor MIMO wireless channels: Models and performance prediction," *IEEE Trans. Comm.*, vol. 50, no. 12, pp. 1926–1934, Dec. 2002.

[10] R. U. Nabar, H. Bölcskei, V. Erceg, D. Gesbert, and A. J. Paulraj, "Performance of multi-antenna signaling techniques in the presence of polarization diversity," *IEEE Trans. Sig. Proc.*, vol. 50, no. 10, pp. 2553–2562, Oct. 2002.

[11] F. Rashid-Farrokhi, A. Lozano, G. J. Foschini, and R. A. Valenzuela, "Spectral efficiency of wireless systems with multiple transmit and receive antennas," in *Proc. IEEE Int. Symp. on PIMRC*, vol. 1, London, UK, Sept. 2000, pp. 373–377.

[12] D. S. Baum, D. Gore, R. Nabar, S. Panchanathan, K. V. S. Hari, V. Erceg, and A. J. Paulraj, "Measurement and characterization of broadband MIMO fixed wireless channels at 2.5 GHz," in *Proc. IEEE ICPWC*, Hyderabad, India, Dec. 2000, pp. 203–206.

[13] R. Stridh, B. Ottersten, and P. Karlsson, "MIMO channel capacity of a measured indoor radio channel at 5.8 GHz," in *Proc. Asilomar Conf. on Signals, Systems and Computers*, vol. 1, Nov. 2000, pp. 733–737.

[14] J. P. Kermoal, L. Schumacher, P. E. Mogensen, and K. I. Pedersen, "Experimental investigation of correlation properties of MIMO radio channels for indoor picocell scenarios," in *Proc. IEEE VTC*, vol. 1, Sept. 2000, pp. 14–21.

[15] A. L. Swindlehurst, G. German, J. Wallace, and M. Jensen, "Experimental measurements of capacity for MIMO indoor wireless channels," in *Proc. IEEE Signal Proc. Workshop on Signal Processing Advances in Wireless Communications*, Taoyuan, Taiwan, March 2001, pp. 30–33.

[16] P. Kyritsi, "Capacity of multiple input-multiple output wireless systems in an indoor environment," Ph.D. dissertation, Stanford University, Jan. 2002.

[17] D. Chizhik, J. Ling, P. W. Wolniansky, R. A. Valenzuela, N. Costa, and K. Huber, "Multiple-input-multiple-output measurements and modeling in Manhattan," *IEEE J. Sel. Areas Comm.*, vol. 23, no. 3, pp. 321–331, Apr. 2003.

[18] A. Paulraj, R. Nabar, and D. Gore, *Introduction to space-time wireless communications*. Cambridge, UK: Cambridge University Press, May 2003.

[19] A. Goldsmith, *Wireless Communications*. Cambridge University Press, 2004, to be published.

[20] G. J. Foschini and M. J. Gans, "On limits of wireless communications in a fading environment when using multiple antennas," *Wireless Pers. Comm.*, vol. 6, no. 3, pp. 311–335, March 1998.

[21] T. Cover and J. Thomas, *Elements of Information Theory*. New York: Wiley, 1991.

[22] L. H. Ozarow, S. Shamai, and A. D. Wyner, "Information theoretic considerations for cellular mobile radio," *IEEE Trans. Veh. Technol.*, vol. 43, no. 2, pp. 359–378, May 1994.

[23] E. Biglieri, J. Proakis, and S. Shamai, "Fading channels: Information-theoretic and communications aspects," *IEEE Trans. Inf. Theory*, vol. 44, no. 6, pp. 2619–2692, Oct. 1998.

[24] T. L. Marzetta and B. M. Hochwald, "Capacity of a mobile multiple-antenna communication link in Rayleigh flat fading," *IEEE Trans. Inf. Theory*, vol. 45, no. 1, pp. 139–157, Jan. 1999.

[25] O. Oyman, R. U. Nabar, H. Bölcskei, and A. J. Paulraj, "Characterizing the statistical properties of mutual information in MIMO channels," *IEEE Trans. Sig. Proc.*, vol. 51, no. 11, Nov. 2003.

[26] B. M. Hochwald and T. L. Marzetta, "Unitary space-time modulation for multiple antenna communications in Rayleigh fading," *IEEE Trans. Inf. Theory*, vol. 46, pp. 543–564, March 2000.

[27] L. Zheng and D. N. C. Tse, "Communicating on the Grassmann manifold: A geometric approach to the non-coherent multiple antenna channel," *IEEE Trans. Inf. Theory*, vol. 48, no. 2, pp. 359–383, Feb. 2002.

[28] B. M. Hochwald, T. L. Marzetta, T. J. Richardson, W. Sweldens, and R. Urbanke, "Systematic design of unitary space-time constellations," *IEEE Trans. Inf. Theory*, vol. 44, no. 6, pp. 1962–1973, Sept. 2000.

[29] N. Seshadri and J. H. Winters, "Two signaling schemes for improving the error performance of frequency-division-duplex

(FDD) transmission systems using transmitter antenna diversity," *Int. J. Wireless Information Networks*, vol. 1, pp. 49–60, Jan. 1994.

[30] H. Bölcskei and A. J. Paulraj, "Space-frequency coded broadband OFDM systems," in *Proc. IEEE WCNC*, vol. 1, Chicago, IL, Sept. 2000, pp. 1–6.

[31] H. Bölcskei, M. Borgmann, and A. J. Paulraj, "Impact of the propagation environment on the performance of space-frequency coded MIMO-OFDM," *IEEE J. Sel. Areas Comm.*, vol. 21, no. 3, pp. 427–439, April 2003.

[32] P. Stoica and E. Lindskog, "Space-time block coding for channels with intersymbol interference," in *Proc. Asilomar Conf. on Signals, Systems and Computers*, vol. 1, Pacific Grove, CA, Nov. 2001, pp. 252–256.

[33] W. Kuo and M. P. Fitz, "Design and analysis of transmitter diversity using intentional frequency offset for wireless communications," *IEEE Trans. Veh. Tech.*, vol. 46, no. 4, pp. 871–881, Nov. 1997.

[34] E. Viterbo and J. Buotros, "A universal lattice code decoder for fading channels," *IEEE Trans. Inf. Theory*, vol. 45, pp. 1639–1642, July 1999.

[35] O. Damen, A. Chkeif, and J. C. Belfiore, "Lattice code decoder for space-time codes," *IEEE Comm. Letters*, vol. 4, no. 5, pp. 161–163, May 2000.

[36] B. Hassibi and H. Vikalo, "On the expected complexity of sphere decoding," in *Proc. Asilomar Conf. on Signals, Systems and Computers*, vol. 2, Nov. 2001, pp. 1051–1055.

[37] U. Fincke and M. Pohst, "Improved methods for calculating vectors of short length in a lattice, including a complexity analysis," *Mathematics of Computation*, vol. 44, pp. 463–471, April 1985.

[38] J. H. Winters, J. Salz, and R. D. Gitlin, "The impact of antenna diversity on the capacity of wireless communications systems," *IEEE Trans. Comm.*, vol. 42, no. 2, pp. 1740–1751, Feb. 1994.

[39] D. Gore, R. W. Heath, and A. Paulraj, "On performance of the zero forcing receiver in presence of transmit correlation," in *Proc. IEEE ISIT*, Lausanne, Switzerland, July 2002, p. 159.

[40] S. Loyka and F. Gagnon, "Performance analysis of the V-BLAST algorithm: An analytical approach," in *Proc. International Zurich Seminar on Broadband Communications*, Feb. 2002, pp. 5.1–5.6.

[41] P. W. Wolniansky, G. J. Foschini, G. D. Golden, and R. A. Valenzuela, "V-BLAST: An architecture for realizing very high data rates over the rich-scattering wireless channel," in *Proc. URSI ISSSE*, Sept. 1998, pp. 295–300.

[42] G. D. Golden, G. J. Foschini, R. A. Valenzuela, and P. W. Wolniansky, "Detection algorithm and initial laboratory results using V-BLAST space-time communication architecture," *Electronic Letters*, vol. 35, no. 1, pp. 14–16, Jan. 1999.

[43] L. Zheng and D. N. C. Tse, "Diversity and multiplexing: A fundamental tradeoff in multiple-antenna channels," *IEEE Trans. Inf. Theory*, vol. 49, no. 5, pp. 1073–1096, May 2003.

[44] W. Jakes, *Microwave Mobile Communications*. New York, NY: Wiley, 1974.

[45] C. B. Papadias and G. J. Foschini, "On the capacity of certain space-time coding schemes," *EURASIP Journal on Applied Signal Processing*, vol. 5, pp. 447–458, May 2002.

[46] S. Sandhu and A. Paulraj, "Space-time block codes: A capacity perspective," *IEEE Comm. Letters*, vol. 4, no. 12, pp. 384–386, Dec. 2000.

[47] G. G. Raleigh and J. M. Cioffi, "Spatio-temporal coding for wireless communication," *IEEE Trans. Comm.*, vol. 46, no. 3, pp. 357–366, March 1998.

[48] D. Agarwal, V. Tarokh, A. Naguib, and N. Seshadri, "Space-time coded OFDM for high data rate wireless communication over wideband channels," in *Proc. IEEE VTC*, vol. 3, May 1998, pp. 2232–2236.

[49] S. Mudulodu and A. Paulraj, "A transmit diversity scheme for frequency selective fading channels," in *Proc. IEEE GLOBECOM*, vol. 2, San Francisco, CA, Nov./Dec. 2000, pp. 1089–1093.

[50] B. Lu and X. Wang, "Space-time code design in OFDM systems," in *Proc. IEEE GLOBECOM*, vol. 2, San Francisco, CA, Nov./Dec. 2000.

[51] B. Lu, X. Wang, and K. Narayanan, "LDPC-based space-time coded OFDM systems over correlated fading channels: Performance analysis and receiver design," *IEEE Trans. Comm.*, vol. 50, no. 1, pp. 74–88, Jan. 2002.

[52] H. Bölcskei and A. J. Paulraj, "Space-frequency codes for broadband fading channels," in *Proc. IEEE ISIT*, Washington, DC, June 2001, p. 219.

[53] H. Bölcskei, M. Borgmann, and A. J. Paulraj, "Space-frequency coded MIMO-OFDM with variable multiplexing-diversity tradeoff," in *Proc. IEEE ICC*, vol. 4, May 2003, pp. 2837–2841.

[54] J. Kim, L. J. Cimini, and J. C. Chuang, "Coding strategies for OFDM with antenna diversity high-bit-rate mobile data applications," in *Proc. IEEE VTC*, vol. 2, May 1998, pp. 763–767.

[55] L. Lang, L. J. Cimini, and J. C. Chuang, "Turbo codes for OFDM with antenna diversity," in *Proc. IEEE VTC*, vol. 2, May 1999, pp. 1664 –1668.

Arogyaswami J. Paulraj (F'91) received the Ph.D. degree from the Naval Engineering College and the Indian Institute of Technology, New Delhi, India.

He is a Professor with the Department of Electrical Engineering, Stanford University, where he supervises the Smart Antennas Research Group, working on applications of space-time techniques for wireless communications. His nonacademic positions included Head, Sonar Division, Naval Oceanographic Laboratory, Cochin, India; Director, Center for Artificial Intelligence and Robotics, Bangalore, India; Director, Center for Development of Advanced Computing, Pune, India; Chief Scientist, Bharat Electronics, Bangalore, India; Chief Technical Officer and Founder, Iospan Wireless Inc., Palo Alto, CA. His research has spanned several disciplines, emphasizing estimation theory, sensor signal processing, parallel computer architectures/algorithms and space-time wireless communications. His engineering experience has included development of sonar systems, massively parallel computers, and more recently broadband wireless systems.

Dr. Paulraj has won several awards for his engineering and research contributions. He is the author of over 280 research papers and holds eight patents. He is a Member of the Indian National Academy of Engineering.

Dhananjay Gore received the B. Tech degree from the Indian Institute of Technology, Bombay (IITB), India, in 1998 and the M.S. and Ph.D. degrees from Stanford University, Stanford, CA, in 2000 and 2003, respectively, all in electrical engineering.

Since May 2003, he has been with Qualcomm Inc., San Diego, CA. His research interests are in signal processing for high-speed wireless communications, smart antennas, and MIMO wireless.

Dr. Gore was a recipient of the Institute Silver Medal from IITB and the School of Engineering Fellowship from Stanford University.

Rohit U. Nabar (S'02) was born in Bombay, India on December 18, 1976. He received the B.S. degree (*summa cum laude*) in electrical engineering from Cornell University, Ithaca, NY, in 1998 and the M.S. and Ph.D. degrees in electrical engineering from Stanford University, Stanford, CA, in 2000, and 2003, respectively. His doctoral research focused on signaling for real-world MIMO channels.

He is currently a postdoctoral research assistant with the Communication Theory Group, Swiss Federal Institute of Technology (ETH), Zürich, Switzerland. His research interests include signal processing and information theory for wireless communications, MIMO wireless systems, and *ad hoc* wireless networks.

Dr. Nabar was a recipient of the Dr. T. J. Rodgers Stanford Graduate Fellowship.

Helmut Bölcskei (M'98–SM'02) was born in Austria on May 29, 1970. He received the Dr. techn. degree in electrical engineering from Vienna University of Technology, Vienna, Austria, in 1997. In 1998 he was a post-doctoral researcher at Vienna University of Technology. From 1999 to 2001 he was a postdoctoral researcher in the Information Systems Laboratory, Department of Electrical Engineering, Stanford University, Stanford, CA. During that period he was also a consultant for Iospan Wireless Inc. From 2001 to 2002 he was an Assistant Professor of Electrical Engineering at the University of Illinois at Urbana-Champaign. Since 2002 he has been an assistant professor of communication theory at ETH Zurich. He was a visiting researcher at Philips Research Laboratories Eindhoven, The Netherlands, ENST Paris, France, and the Heinrich Hertz Institute Berlin, Germany. His research interests include communication and information theory with special emphasis on wireless communications.

He received a 2001 IEEE Signal Processing Society Young Author Best Paper Award and was an Erwin Schrödinger Fellow (1999-2001) of the Austrian National Science Foundation (FWF). He serves as an associate editor for the IEEE Transactions on Wireless Communications, the IEEE Transactions on Signal Processing, and the EURASIP Journal on Applied Signal Processing.

Figure Captions

Fig. 1. Bandwidth requirement and range of a 1Gbps link using MIMO technology.

Fig. 2. Schematic of wavefront impinging on an antenna array. Under the narrowband assumption the antenna outputs $y_1(t)$ and $y_2(t)$ are identical except for a phase shift.

Fig. 3. Construction of the MIMO channel model from a physical scattering description.

Fig. 4. Measured time-frequency response of an $M_T = 2, M_R = 2$ MIMO channel. $H_{i,j}$ denotes the scalar sub-channel between the j-th transmit and the i-th receive antenna.

Fig. 5. Ergodic capacity for different MIMO antenna configurations. Note that the SIMO channel has a higher ergodic capacity than the MISO channel.

Fig. 6. 10% outage capacity for different MIMO configurations. MIMO yields significant improvements in terms of outage capacity.

Fig. 7. The capacity of a frequency-selective fading MIMO channel is the sum of (appropriately normalized) capacities of frequency-flat fading MIMO sub-channels.

Fig. 8. CDF of the mutual information of an increasingly frequency-selective fading MIMO channel. Outage performance improves with frequency-selective fading, due to increased frequency diversity.

Fig. 9. Generic coding architecture for MIMO channels.

Fig. 10. Schematic of the transmission strategy for the Alamouti scheme. The MISO channel is orthogonalized irrespectively of the channel realization.

Fig. 11. Comparison of the (uncoded) symbol error rate of the Alamouti scheme ($M_T = 2, M_R =$

1) *with receive diversity* $(M_T = 1, M_R = 2)$. *Both schemes achieve the same diversity order of two (reflected by the slope of the error rate curve), but receive diversity realizes an additional 3dB receive array gain (reflected by the offset of the error rate curve).*

Fig. 12. *Schematic of delay diversity – a space selective MISO channel is converted into a frequency-selective SISO channel.* T_s *denotes a delay of one symbol period.*

Fig. 13. *Schematic of horizontal encoding (HE) for spatial multiplexing. This is a sub-optimal encoding technique that realizes at most* M_R*-th order diversity but simplifies receiver design.*

Fig. 14. *Schematic of vertical encoding (VE) for spatial multiplexing. VE spreads the information bits across all transmit antennas realizing* $M_T M_R$*-th order diversity at higher decoding complexity compared to HE.*

Fig. 15. *Schematic of a linear receiver front-end to separate the transmitted data streams over a MIMO channel.*

Fig. 16. *Comparison of ML, OSUC, SUC and MMSE receivers over an i.i.d. MIMO channel. OSUC is superior to SUC and MMSE.*

Fig. 17. *PER vs. SNR for a transmission rate of 6bps/Hz over an i.i.d. MIMO channel with* $M_T = M_R = 2$.

Fig. 18. *Rate vs. SNR for a fixed PER of 10% over an i.i.d. MIMO channel with* $M_T = M_R = 2$.

Fig. 19. *Signaling limit surface (Rate vs. PER vs. SNR) for optimal coding over* $\mathbf{H}_w$ *MIMO channel with* $M_T = M_R = 2$. *Vertical contour lines are at constant SNR, horizontal contour lines are at constant PER.*

Fig. 20. *Signaling limit surface (Rate vs. PER vs. SNR) for OSTBC and for SM-HE with MMSE front-end over an i.i.d. MIMO channel with* $M_T = M_R = 2$.

Fig. 21. PER vs. SNR at fixed transmission rate of 6bps/Hz for OSTBC (Alamouti scheme) and SM-HE with MMSE front-end, over an i.i.d. MIMO channel with $M_T = M_R = 2$.

Fig. 22. Schematic of OFDM transmission for a SISO channel.

Table Captions

Table I. Performance features of receivers for uncoded spatial multiplexing. SNR loss is with respect to the ML receiver.

Receiver	Diversity Order	SNR Loss
ZF	$M_R - M_T + 1$	High
MMSE	$\approx M_R - M_T + 1$	Low
SUC	$\approx M_R - M_T + 1$	Low
OSUC	$> M_R - M_T + 1, \ < M_R$	Low
ML	M_R	Zero

TABLE I
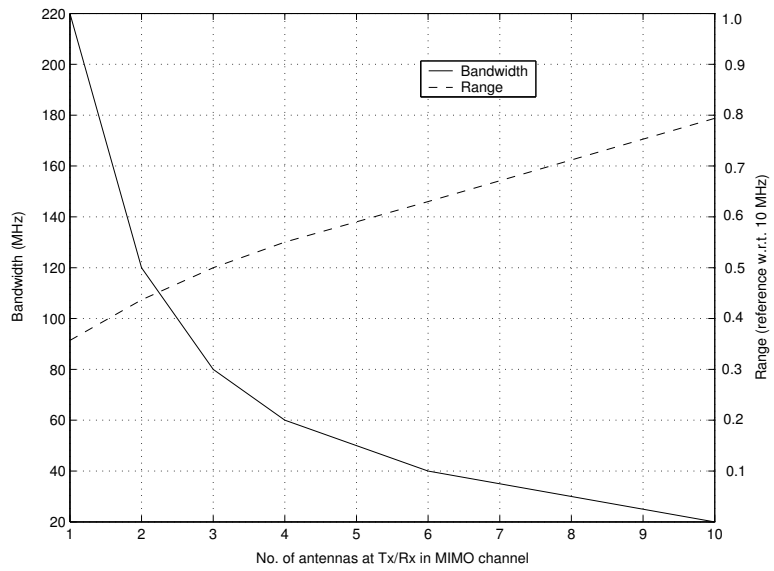
Fig. 1.
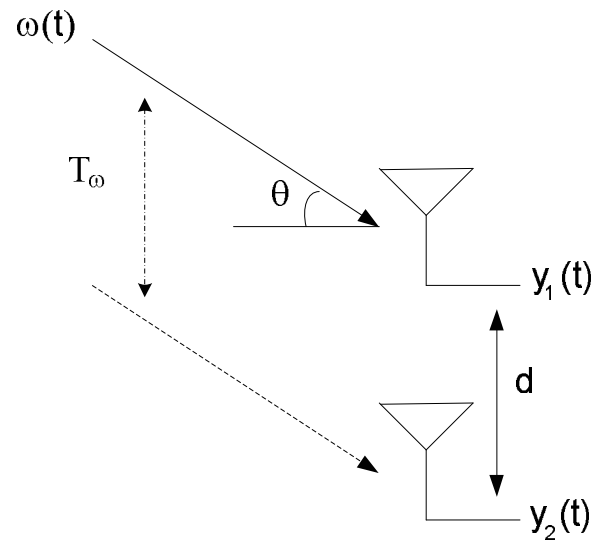
Fig. 2.
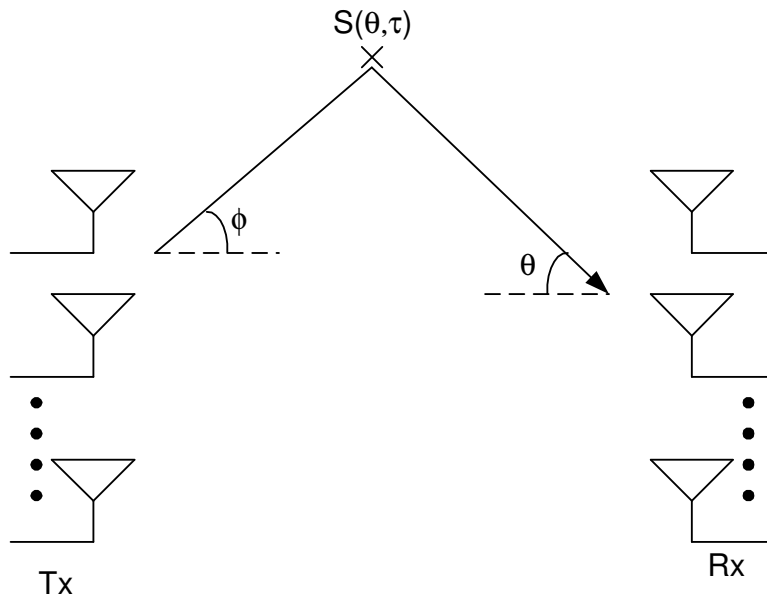
Fig. 3.

Fig. 4.

Fig. 5.

Fig. 6.

Fig. 7.

Fig. 8.

qK bits

Temporal Coding +
Symbol Mapping +
Interleaving

N Symbols

Space-Time
Coding

M_T

T

Space-Time
Codeword

Fig. 9.

Symbol period 2 $-s_2^*$ s_1^*

Symbol period 1 s_1 s_2

Tx 1   Tx 2

h_1 h_2

Rx

Fig. 10.

Fig. 11.

Fig. 12.

$\dfrac{qK}{M_T}$

Temporal Coding + Symbol Mapping + Interleaving

$\dfrac{N}{M_T}$ symbols

qK bits

$1 : M_T$ Demultiplexing

$\dfrac{qK}{M_T}$

Temporal Coding + Symbol Mapping + Interleaving

$\dfrac{N}{M_T}$ symbols

$T = \dfrac{N}{M_T}$

M_T
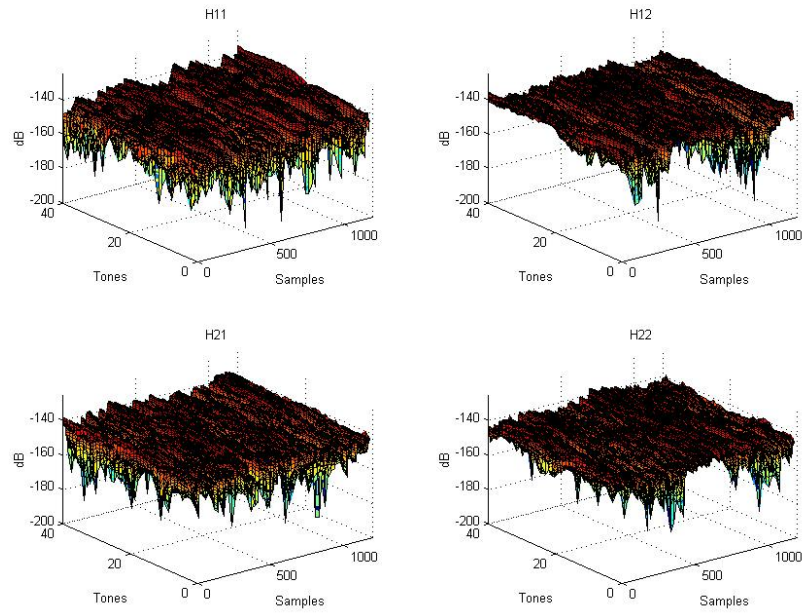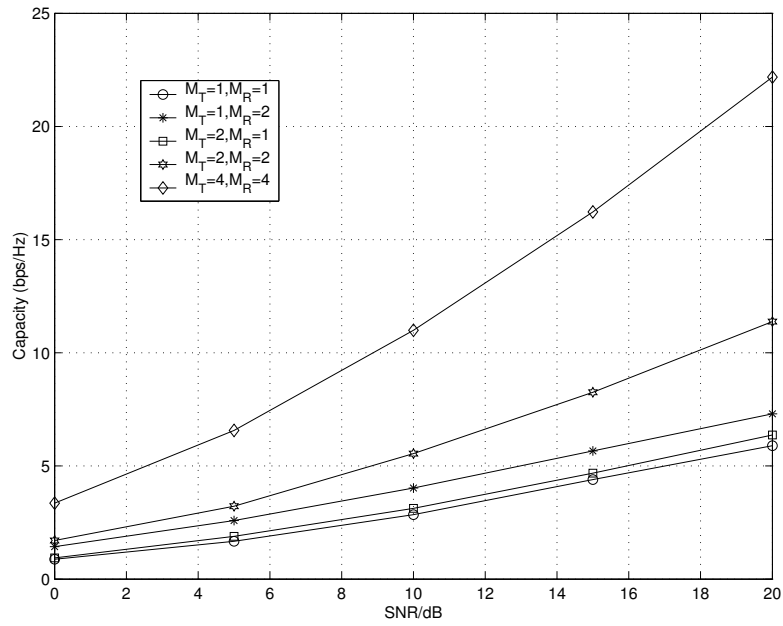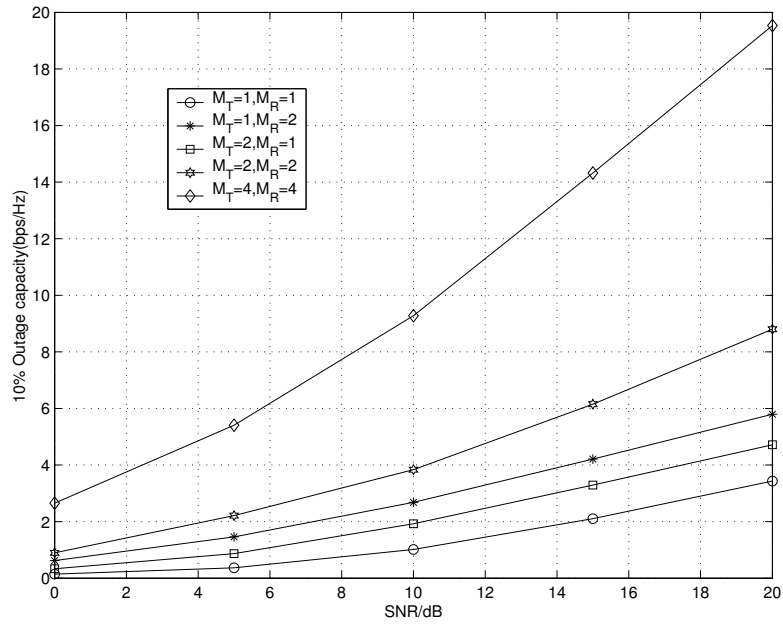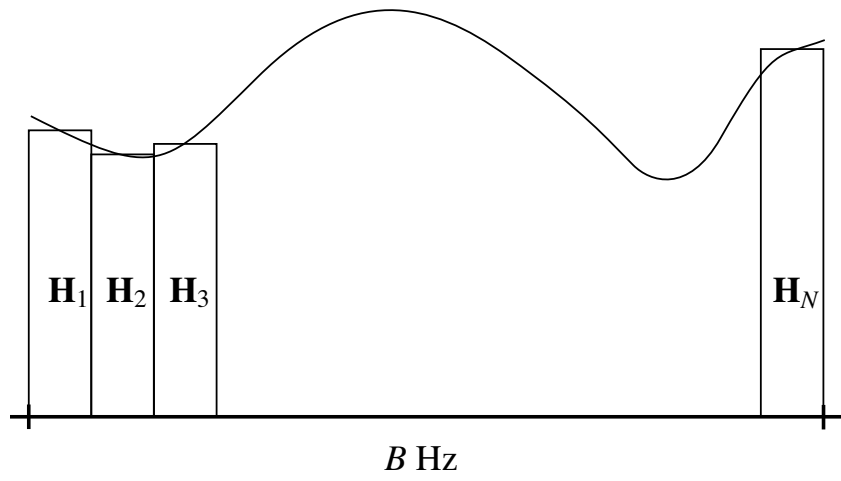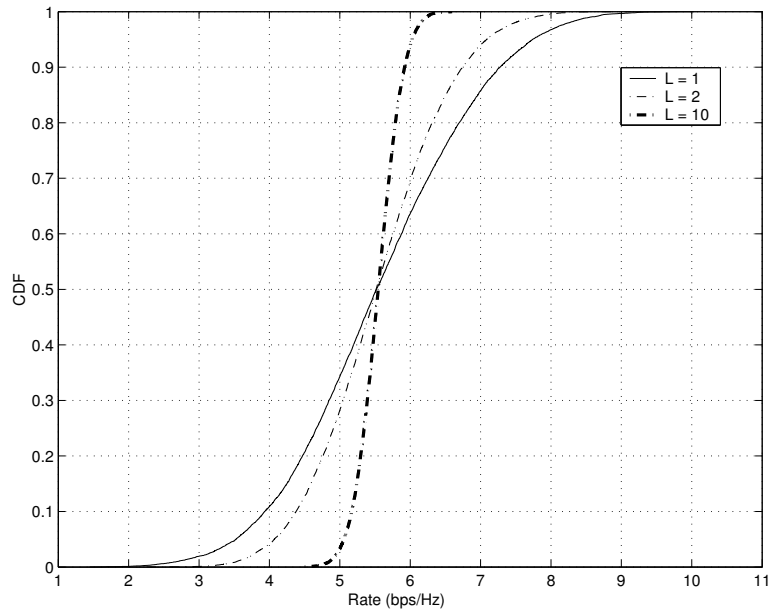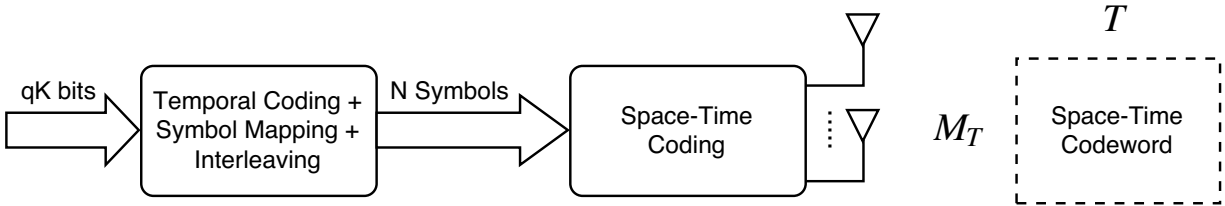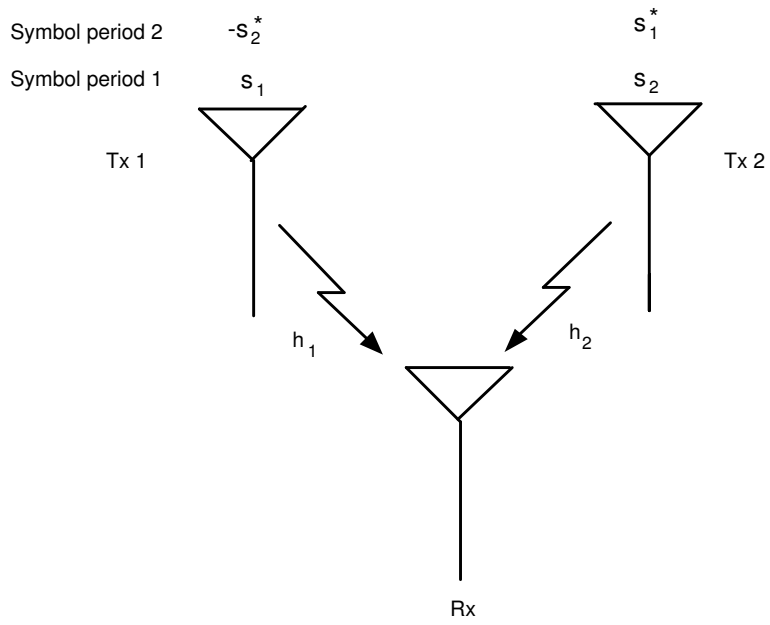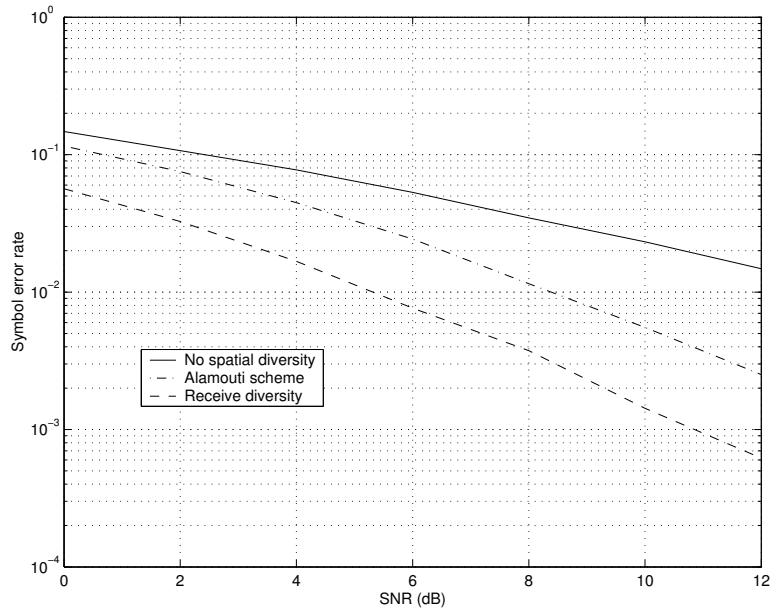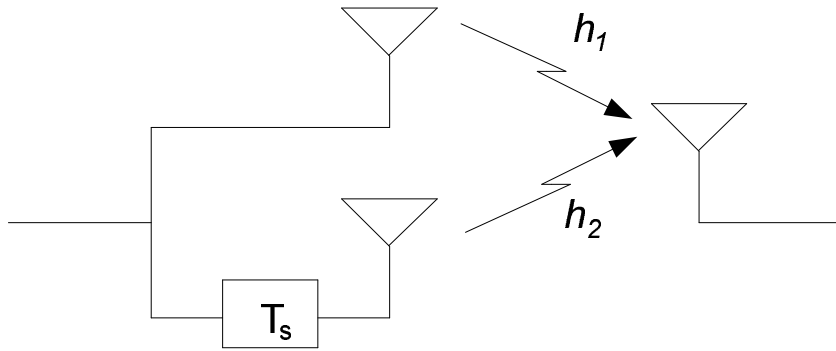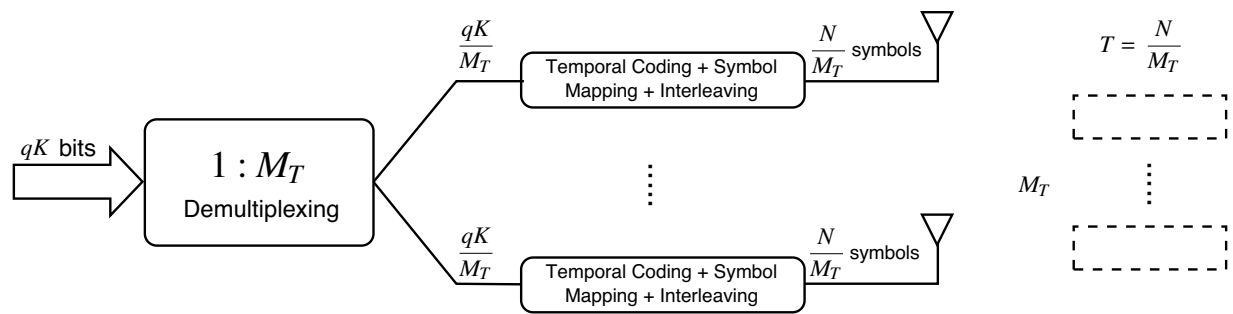
Fig. 13.
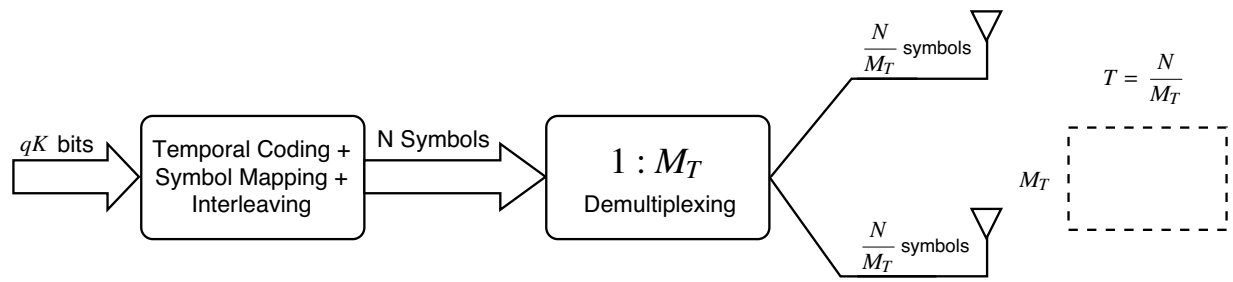
Fig. 14.
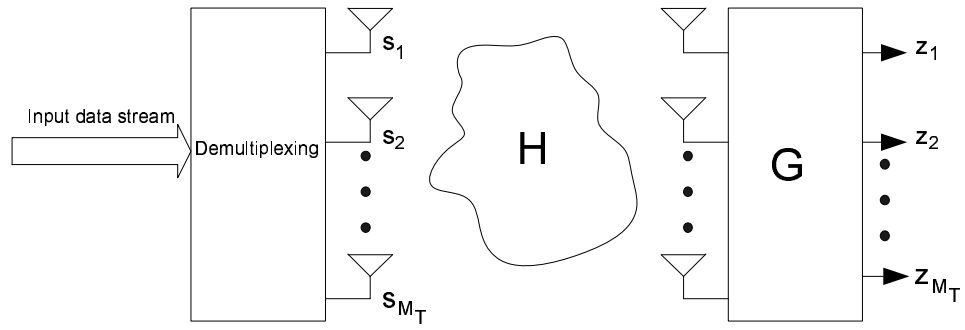
Fig. 15.
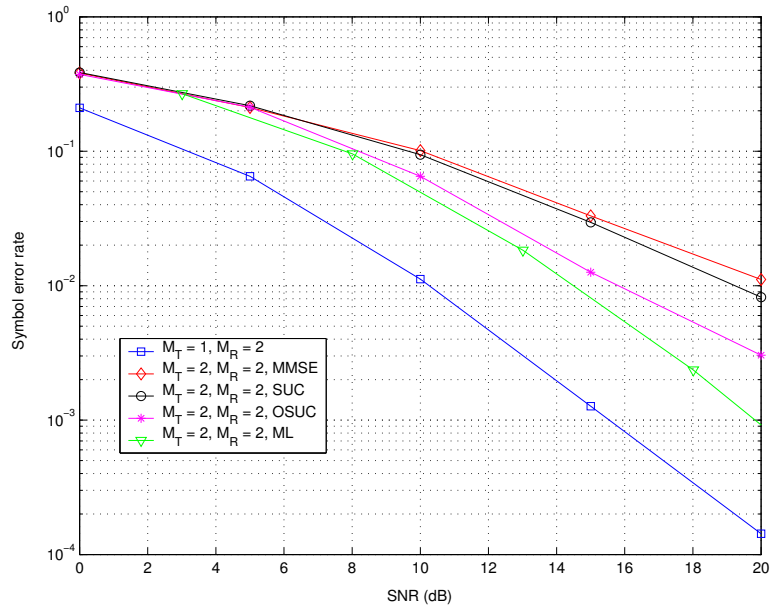
Fig. 16.
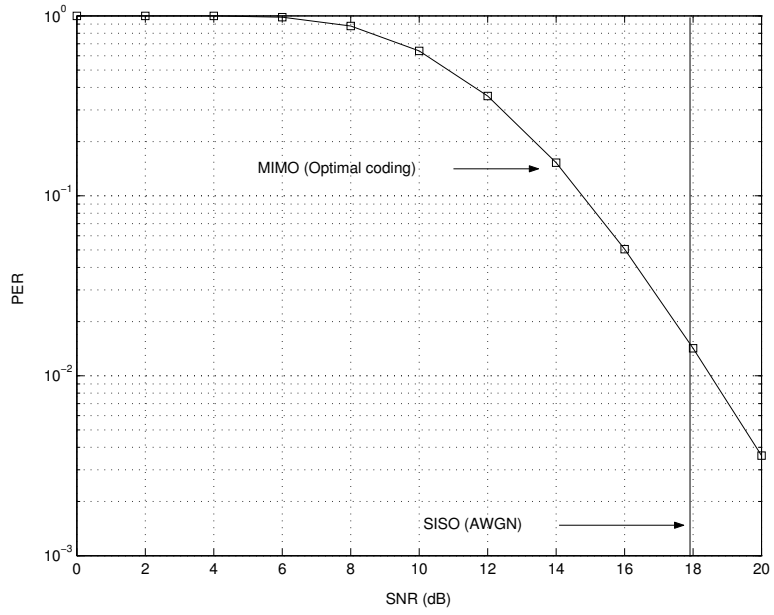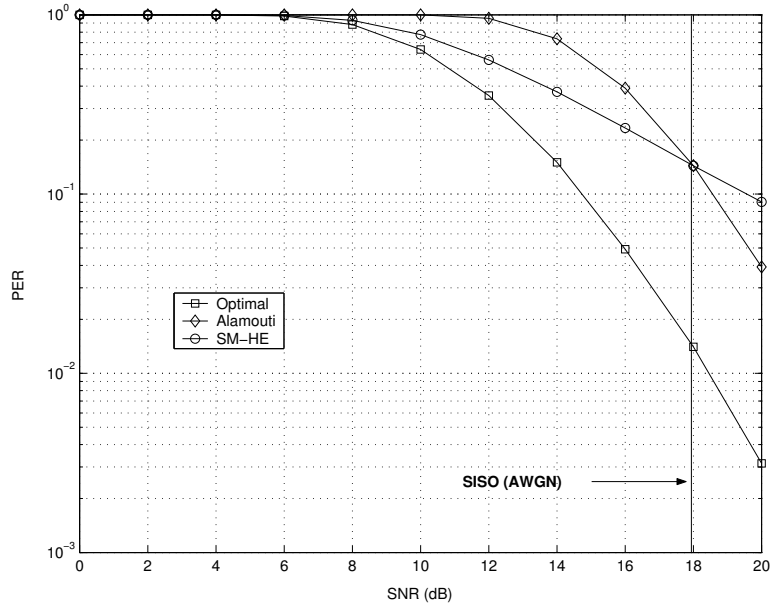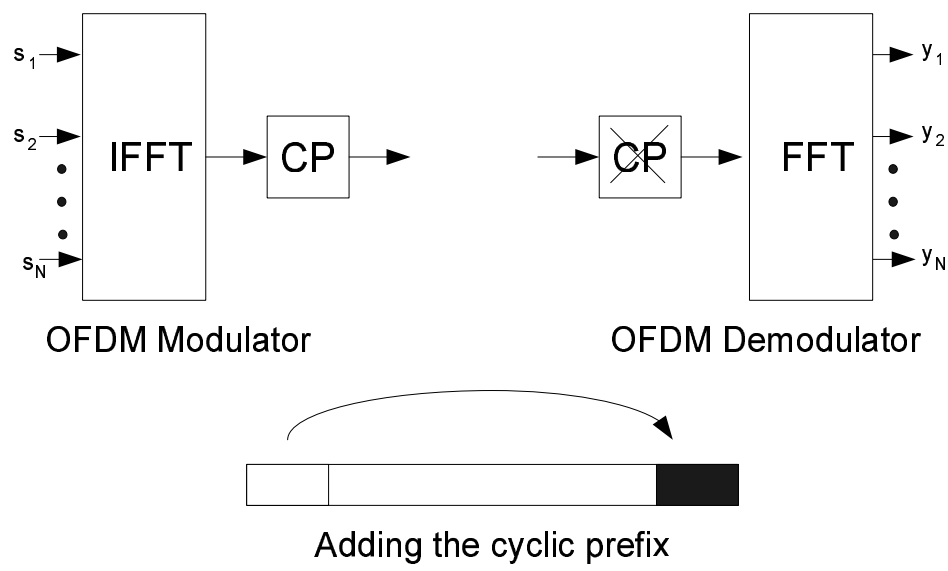
Fig. 17.
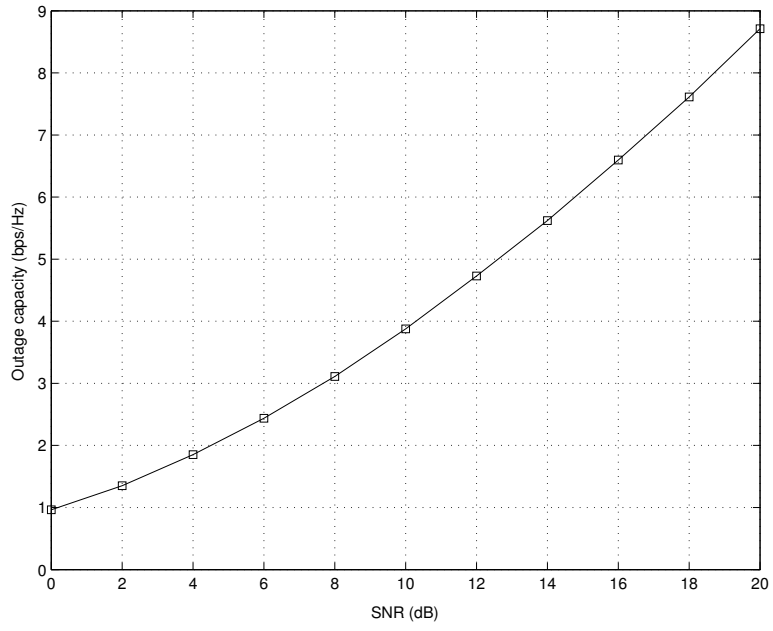
Fig. 18.
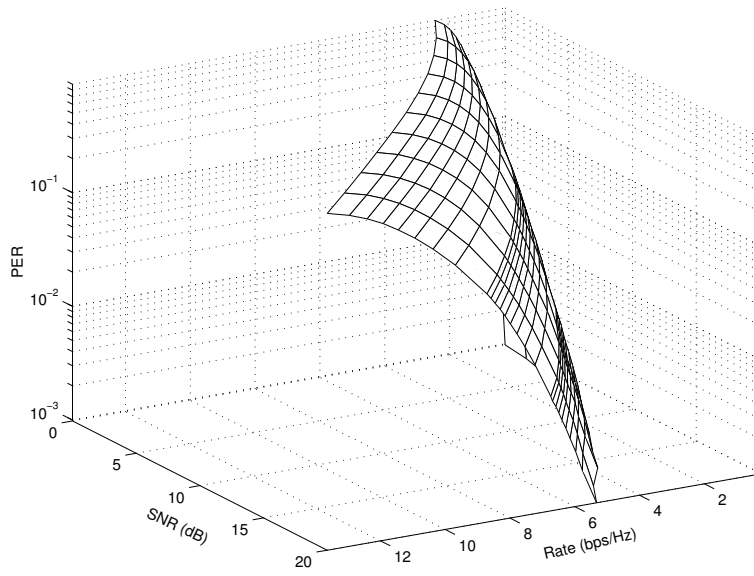
Fig. 19.
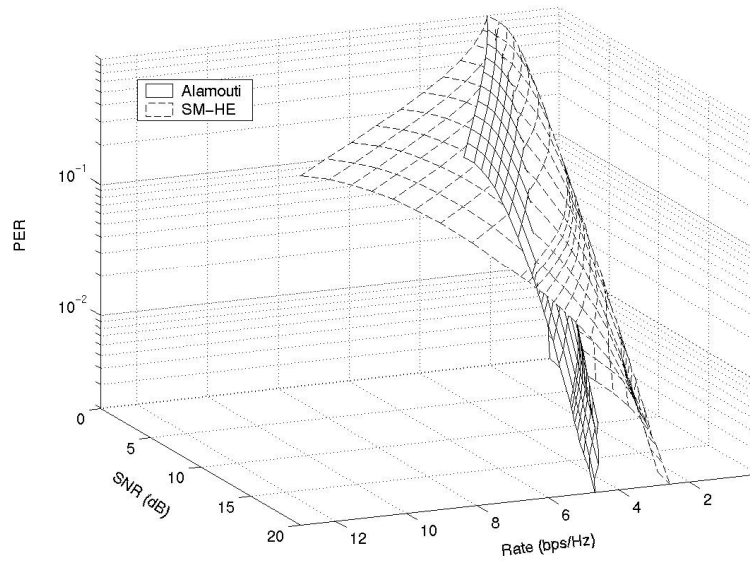
Fig. 20.

Fig. 21.

Fig. 22.

Affiliation and Contact Information for all Authors

Arogyaswami J. Paulraj

Affiliation: Information Systems Laboratory, Stanford University, Stanford, CA

Address: 272 Packard, 350 Serra Mall, Stanford, CA 94305

Phone: +1-650-725-8307; Fax:+1-650-723-8473; E-mail: apaulraj@stanford.edu

Dhananjay Gore

Affiliation: Qualcomm Inc., San Diego, CA

Address: AM-155P, 9940 Barnes Canyon Road, San Diego, CA 92121

Phone: +1-858-658-2649; Fax:+1-858-845-2651; E-mail: dgore@qualcomm.com

Rohit U. Nabar

Affiliation: Communication Technology Laboratory, Swiss Federal Institute of Technology (ETH)

Zürich, Switzerland

Address: ETF E119, Sternwartstrasse 7, CH-8092 Zürich, Switzerland

Phone: +41-1-63-23081; Fax: +41-1-63-21209; E-mail: nabar@nari.ee.ethz.ch

Helmut Bölcskei

Affiliation: Communication Technology Laboratory, Swiss Federal Institute of Technology (ETH)

Zürich, Switzerland

Address: ETF E122, Sternwartstrasse 7, CH-8092 Zürich, Switzerland

Phone: +41-1-63-23433; Fax: +41-1-63-21209; E-mail: boelcskei@nari.ee.ethz.ch